北京理工大學
BEIJING INSTITUTE OF TECHNOLOGY

# Crystal Growth and Physical Properties Manipulation of Quantum Materials

**Zhiwei Wang**

School of Physics, Beijing Institute of Technology

email: zhiweiwang@bit.edu.cn






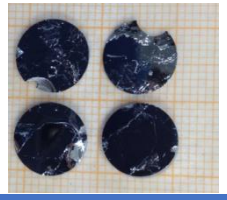
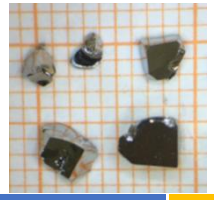

# Outline

北京理工大學 BEIJING INSTITUTE OF TECHNOLOGY

- 1. Introduction of crystal and crystal growth
- 2. Crystal growth, physical properties of Kagome superconductors $AV_3Sb_5$
- 3. Exploration of topological superconductors
- 4. Summary

# Outline

北京理工大學 BEIJING INSTITUTE OF TECHNOLOGY

- 1. Introduction of crystal and crystal growth
- 2. Crystal growth, physical properties of Kagome superconductors $AV_3Sb_5$
- 3. Exploration of topological superconductors
- 4. Summary

# 1 Crystals in our daily life

北京理工大學 BEIJING INSTITUTE OF TECHNOLOGY

Rock sugar

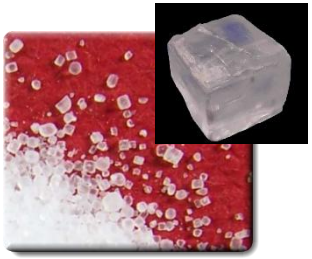

Salt (NaCl)

Gourmet powder

Blue vitriol [$CuSO_4 \cdot 5H_2O$]

Diamond (C)

Ruby ($Al_2O_3$)

Sapphire ($Al_2O_3$)

Rock crystal ($SiO_2$)

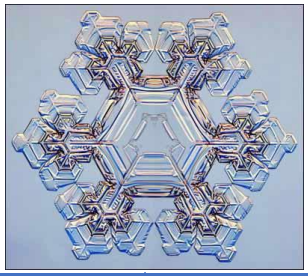

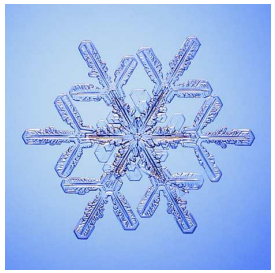

Snowflake ($H_2O$)

# Naturally formed crystals


Diamond (金刚石)


Calcite (方解石)


Fluorite (萤石)


Garnet (石榴子石)


purple crystal
(紫色水晶)


Orange red crystal
(桔红色水晶)


Agate (玛瑙)


Mica (云母)


(pebbles)雨花石


Stone (岩石)


Sand (沙子)


Earth (泥土)

# What is crystal ?

北京理工大學 BEIJING INSTITUTE OF TECHNOLOGY

- Solids in nature can be divided into **crystals, amorphous, and quasicrystals**.

- **Crystal**: The atoms, ions, or molecules that make up a solid are periodically arranged according to a certain crystal structure; It has long-range order, periodicity, symmetry, and a regular shape.

- **Amorphous**: The atoms, ions, or molecules arranged repeatedly without periodic translation; it has a short range order, and without a specific regular shape. For example, glass, plastic, resin, amber, etc

- **Quasicrystal**: A solid between crystal and amorphous. Having a long-range ordered atomic arrangement similar to crystals, but without the translational symmetry of crystals. Having macroscopic symmetry that crystals do not allow

# The relationship between crystal and amorphous



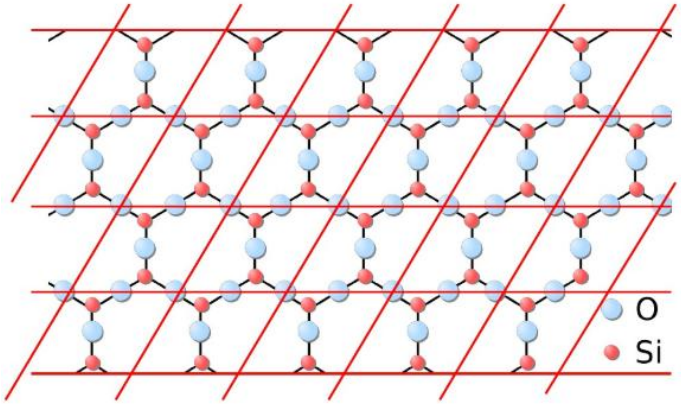


Crystals with long-range ordered

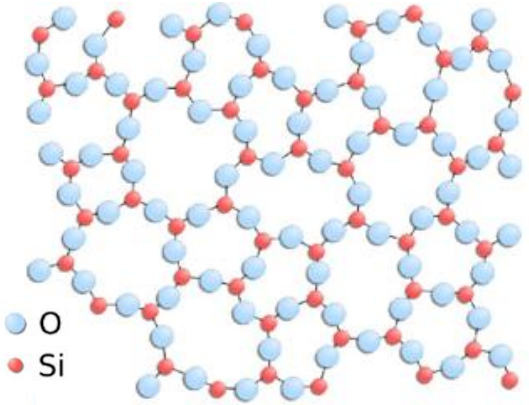


Amorphous with short-range ordered

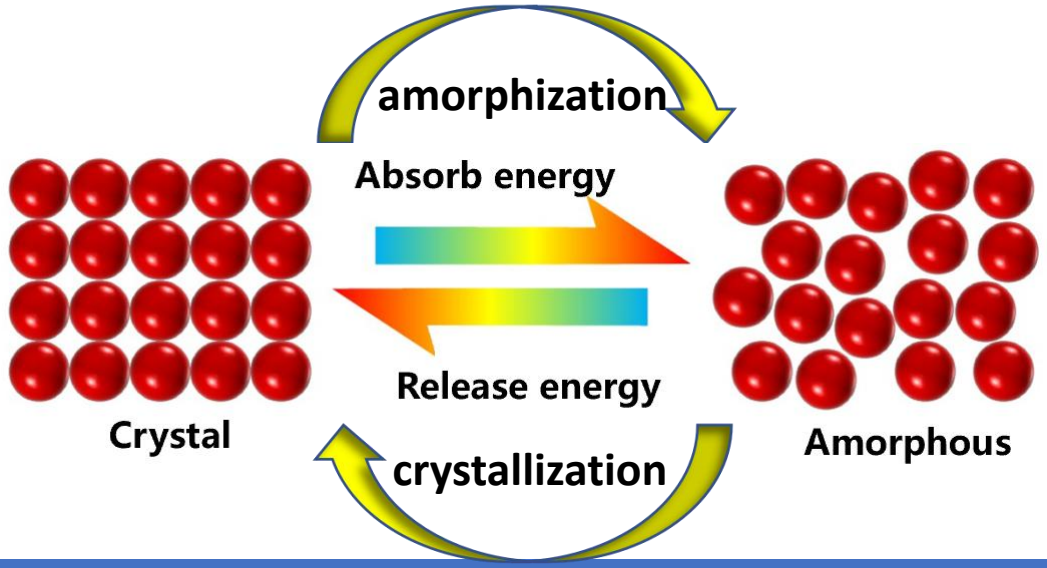


**The crystalline state is the most stable state !!**

# Single crystal and polycrystal

北京理工大學 BEIJING INSTITUTE OF TECHNOLOGY

**Single crystal:** A single crystal is a single particle with a complete crystal shape (crystal edges, complete crystal planes)

**Polycrystal:** There are multiple grains within a particle, and the lattice of each grain is periodically arranged, but the orientation of these grains is arbitrary.

Polycrystal rock sugar

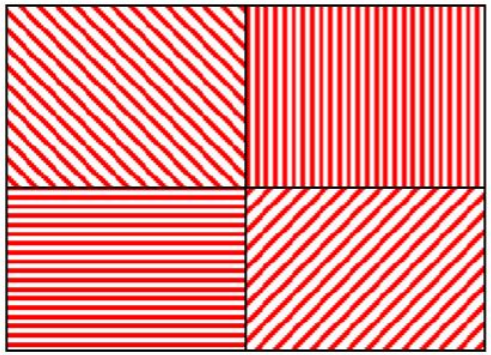

sketch of polycrystal

Polycrystalline corn field

Single crystal rock sugar

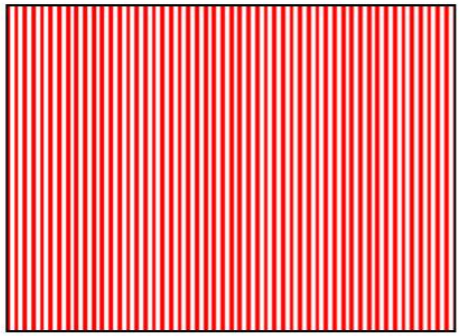

sketch of single crystal

Single crystal corn field

# Quasicrystal



Prof. Daniel Shechtman

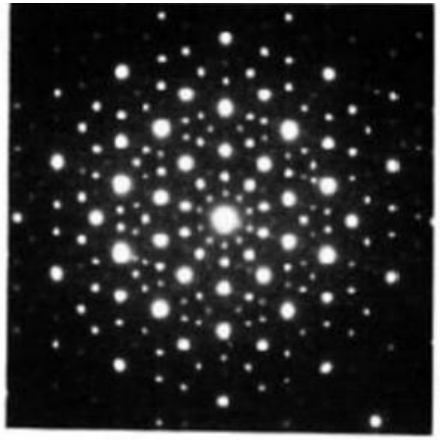

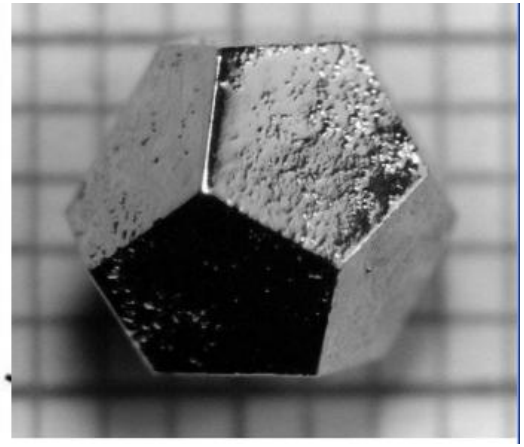

VOLUME 53, NUMBER 20 PHYSICAL REVIEW LETTERS 12 NOVEMBER 1984

**Metallic Phase with Long-Range Orientational Order and No Translational Symmetry**

D. Shechtman and I. Blech
*Department of Materials Engineering, Israel Institute of Technology–Technion, 3200 Haifa, Israel*

and

D. Gratias
*Centre d'Etudes de Chimie Métallurgique, Centre National de la Recherche Scientifique, F-94400 Vitry, France*

and

J. W. Cahn
*Center for Materials Science, National Bureau of Standards, Gaithersburg, Maryland 20760*
(Received 9 October 1984)

We have observed a metallic solid (Al–14-at.%-Mn) with long-range orientational order, but with icosahedral point group symmetry, which is inconsistent with lattice translations. Its diffraction spots are as sharp as those of crystals but cannot be indexed to any Bravais lattice. The solid is metastable and forms from the melt by a first-order transition.

- With long-range ordered atomic arrangement similar to crystals, but without the translational symmetry of crystals; cannot be described by Bravais lattice.
- Daniel Shechtman discovered the quasicrystal in AlMn alloy in 1984, won 2011 Nobel Prize in chemistry

# Summary of crystal, amorphous, and quasicrystal



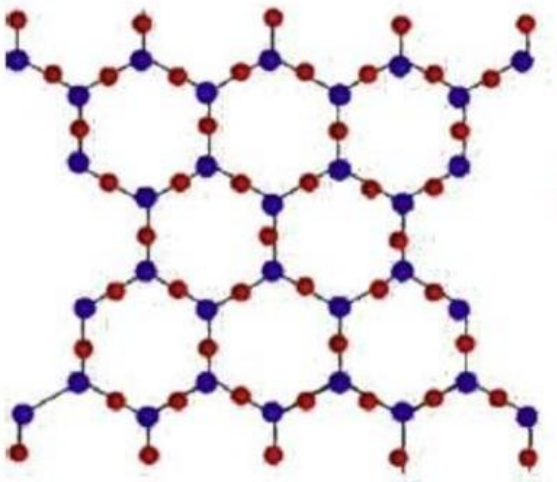

Quartz (crystal)

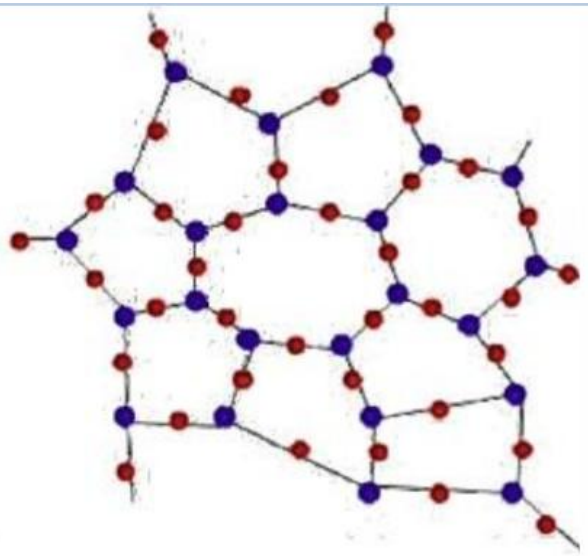

Quartz (glass)

Quasicrystal

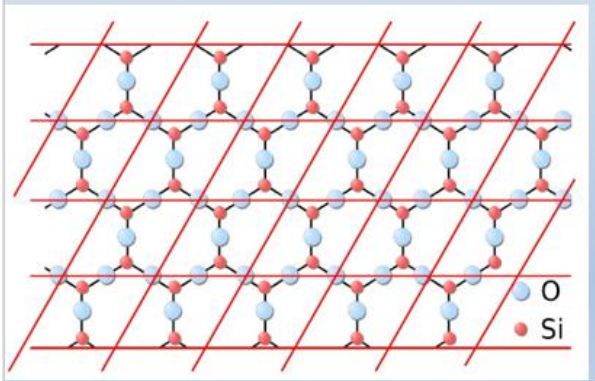


Crystals with long-range ordered

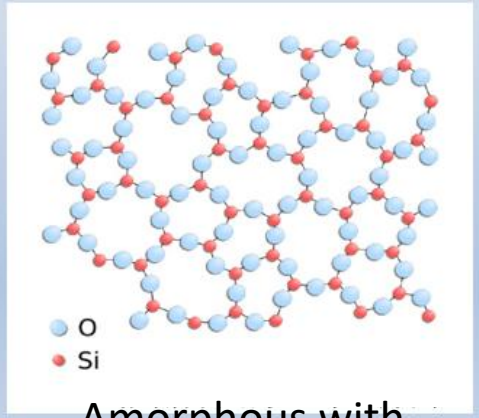


Amorphous with short-range ordered

no translational symmetry


Five-fold symmetry

北京理工大學 BEIJING INSTITUTE OF TECHNOLOGY

## Crystal growth techniques

- 1. solid-solid growth: not common for growing large crystal; popularly used in metallurgical processes.
- 2. vapor-solid growth: sublimation–condensation; sputtering; epitaxial processes; chemical vapor transport……
- 3. liquid-solid growth
  - a. melt growth
  - b. solution growth
  - c. flux growth
  - d. hydrothermal growth

北京理工大學 BEIJING INSTITUTE OF TECHNOLOGY

# Driving force of crystal growth

$\Delta\mu = \mu_m - \mu_c$

$\mu_m$ : chemical potential of a melt, solution, or vapor phase (*the growth medium*)

$\mu_c$ : chemical potential of crystalline phase

When the growth medium is a melt:

the level of supercooling $\Delta T = T_m - T$ becomes the driving force

$\Delta\mu = L\Delta T/T_m$ , $L$ is the latent heat of melting

When the growth medium is a vapor:

the level of supersaturation $\sigma = (p - p_e) / p_e$ becomes the driving force

$$\Delta\mu = k_B T \log(p/p_e) \Rightarrow \Delta\mu = k_B T \log(1+\sigma) \approx k_B T\sigma$$

$k_B$ is Boltzmann's constant

When the growth medium is a solution:

the level of supersaturation $\sigma = (C - C_e) / C_e$ can be defined as the driving force

$$\Delta\mu = k_B T \log(C/C_e) \Rightarrow \Delta\mu = k_B T \log(1+\sigma) \approx k_B T\sigma$$

# 1 Introduction of crystal growth

北京理工大學 BEIJING INSTITUTE OF TECHNOLOGY

three basic steps of the formation of a crystal

- 1. Achievement of supercooling or supersaturation (driving force);
- 2. Nucleation;
- 3. Growth of the nuclei into single crystals of distinct phases

# How to grow crystals in lab

北京理工大學 BEIJING INSTITUTE OF TECHNOLOGY

## Prerequisites for crystal growth

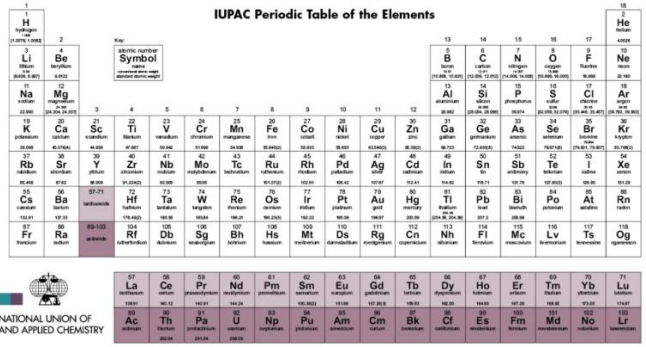


1. Starting materials:
   elements, compounds

2. balance, mortar, crucible, glove box, pump system, etc.


balance


mortar


crucibles


quartz tube


glove box


pump and seal system

3. Facilities for crystal growth


Box furnace


Tube furnace


Float-zone furnace


High-T high-P furnace

# Procedure of crystal growth

北京理工大學 BEIJING INSTITUTE OF TECHNOLOGY

## Taking $TlBi_{1-x}Sb_xTe_2$ as an example

starting materials

- 1. choose starting materials: high pure Tl shots, Bi shots, Sb shots and Te shots, pretreat the starting materials;

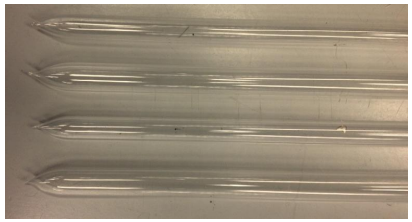
prepared quartz tubes

- 2. prepare the quartz tubes;

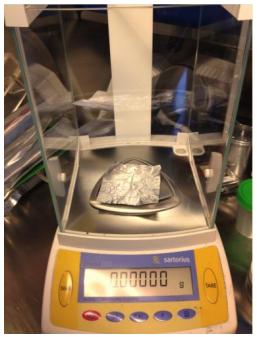
balance

- 3. properly weight according to stoichiometric ratio (manipulate in a Ar-filled glove box);

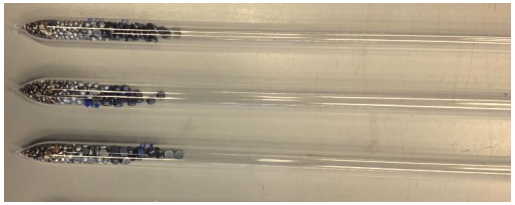
tubes with loaded materials

- 4. load the starting materials into a quartz tube (in a Ar-filled glove box);

# Procedure of crystal growth

北京理工大學 BEIJING INSTITUTE OF TECHNOLOGY

5. evacuate the quartz tube;

Sealing system

Gas cylinders

Hydrogen flame

6. seal the quartz tube;

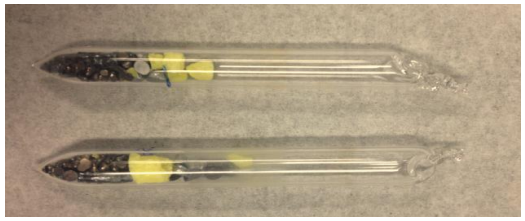

Sealed quartz tubes

7. put the tube into a furnace;

8. set parameters of furnace and start crystal growth.

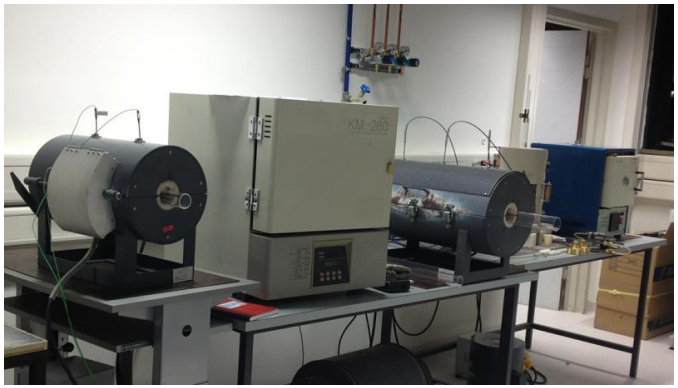

Muffle furnaces and tube furnace

# 1 Introduction of crystal growth

北京理工大學 BEIJING INSTITUTE OF TECHNOLOGY

If you know how to design and grow samples, then you will have the freedom to create samples that allow you to pursue the science that appeals to you: superconductors, topological insulators, magnetic materials, semimetals *etc*.

**If you know how to cook, you can create whatever you want.**

Dumpling

Pizza

Sushi

# (1) Kagome Materials

北京理工大學 BEIJING INSTITUTE OF TECHNOLOGY

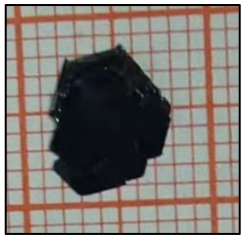

$RbV_3Sb_5$

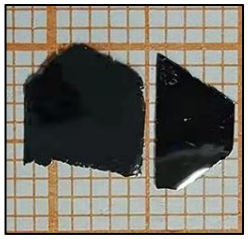

$CsV_3Sb_5$

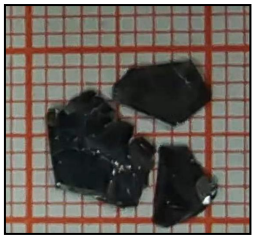

$KV_3Sb_5$

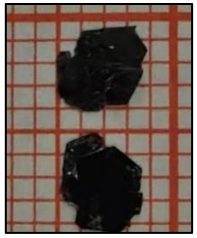

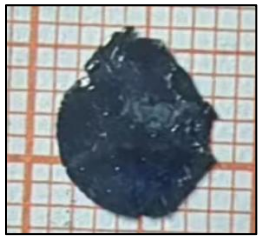

Ta、Mo Nb、Cr and Sn -doped $CsV_3Sb_5$

Flat bands, SC, CDW, AHE

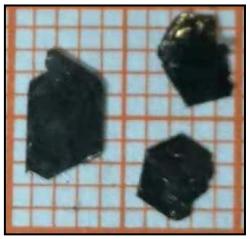

$TbMn_6Sn_6$

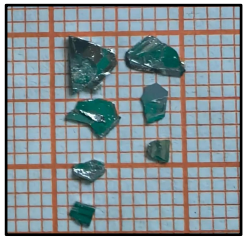

$GdMn_6Sn_6$

$HfMn_6Sn_6$

$ZrMn_6Sn_6$

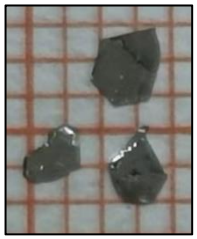

$GdV_6Sn_6$

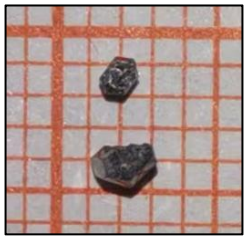

$HfV_6Sn_6$

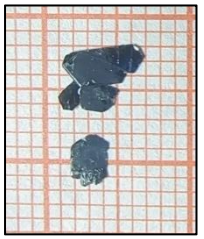

$CsV_6Sb_6$

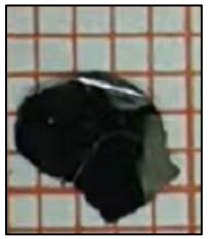

$RbV_6Sb_6$

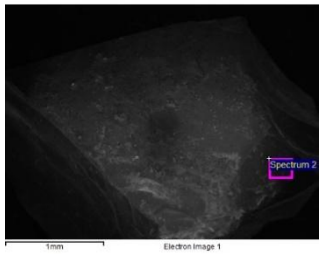


$RbBi_2$

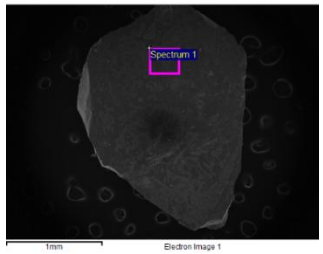


$CsBi_2$

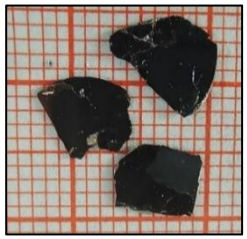

$CsTi_3Bi_5$

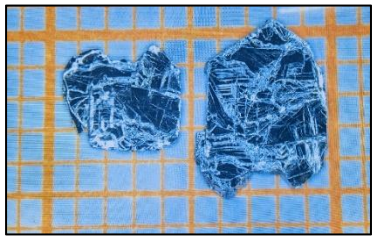

$Pt_3Tl_2$

# (2) Magnetic Materials

北京理工大學 BEIJING INSTITUTE OF TECHNOLOGY

## 反铁磁性拓扑材料

$EuIn_2As_2$

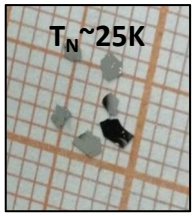

$EuIn_2P_2$

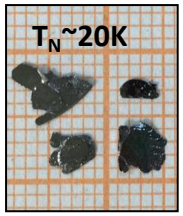

$MnBi_2Te_4$

$MnBi_4Te_7$

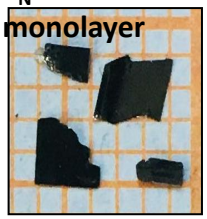

$TaCoTe_2$

CuMnAs

$Eu_5In_2Bi_6$

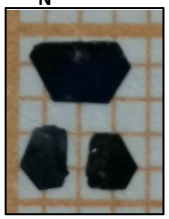

$Co_{1/3}NbS_2$

$Co_{1/3}TaS_2$

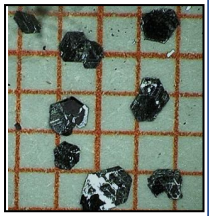
PdCoO2

## 铁磁性拓扑材料

$Co_3Sn_2S_2$

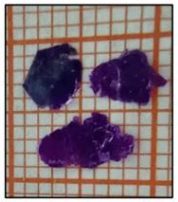
$CrCl_3$

$Co_{0.8}V_{0.2}Sn$

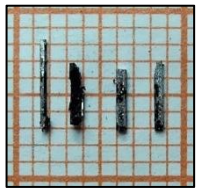

$Co_{0.6}Mn_{0.4}Sn$

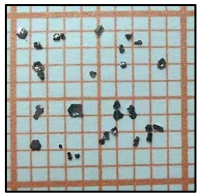

$Fe_3Sn_2$

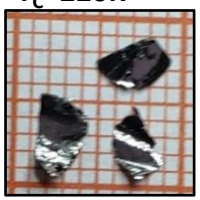

$Fe_3GeTe_2$


$EuSn_2As_2$

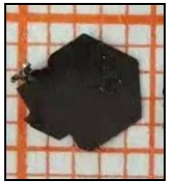

$Fe_5GeTe_2$


$Cr_2Ge_2Te_6$

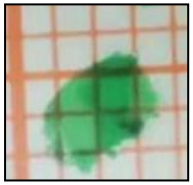

$CoBr_2$

$Co_2S_2Tl$

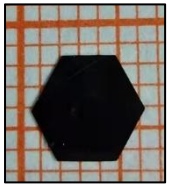

$K_{0.5}RhO_2$

PrAlSi

PrAlGe

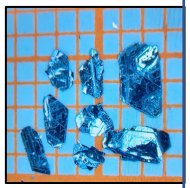

$Fe_3GaTe_2$

## 多重磁性拓扑材料

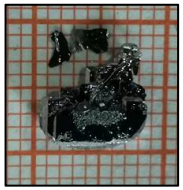
NdAlSi


NdAlGe

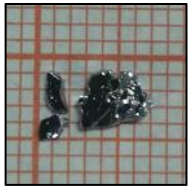
$EuAl_4$

# (3) Quantum materials with layered structure

北京理工大學 BEIJING INSTITUTE OF TECHNOLOGY

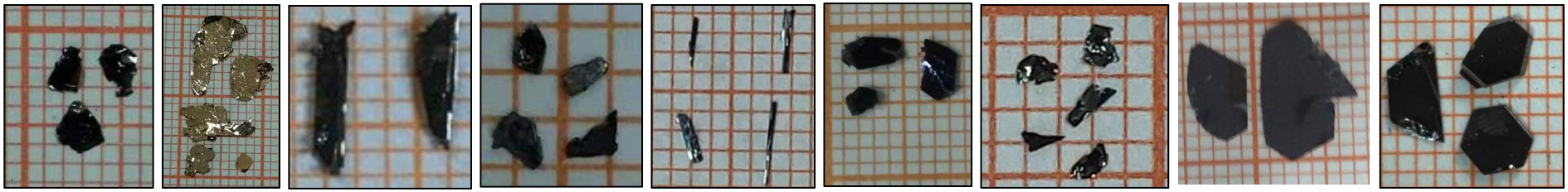

$ZrTe_2$ Dirac SM | $LaTe_3$ CDW | $Ta_2NiSe_5$ exciton insulator | $LaOBiS_2$ FE | $TaSe_2$ CDW SC | $Pd_3P_2S_8$ Flat bands | $Nb_3TeCl_7$ Flat bands | $Nb_3Cl_8$ Flat bands | $TiSe_2$ CDW SC

GeSe | $2H\text{-}MoTe_2$ | $2H\text{-}WSe_2$ | $CrI_3$ | $Ta_2Pd_3Te_5$ | $Ta_2Ni_3Te_5$ | $TaCo_2Te_2$ | $Nb_3I_8$ Flat bands

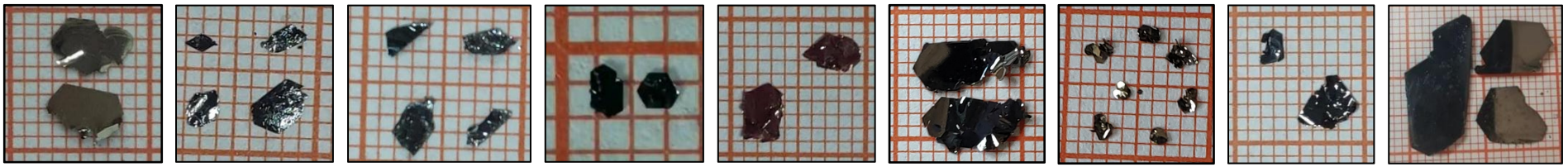

$1T\text{-}TaS_2$ | $In_2Se_3$ | InSe | $ZrS_2$ | GaSe | $FePS_3$ | $NiPS_3$ | $CoPS_3$ | $TiTe_2$

# (3) Quantum materials with layered structure

北京理工大學 BEIJING INSTITUTE OF TECHNOLOGY

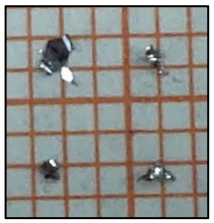
$ReS_2$


$ReSe_2$


$Pt_2TlTe_3$

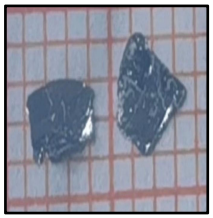
$Pt_2TlTe_2Se$

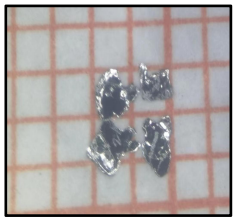
$Pt_2TlTeSe_2$

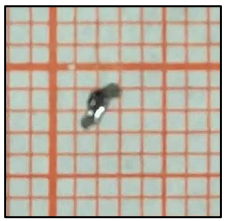
$Pt_2TlSe_3$

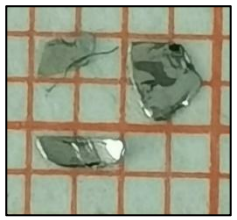
$BiI_3$

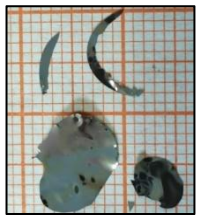
$VTe_2$

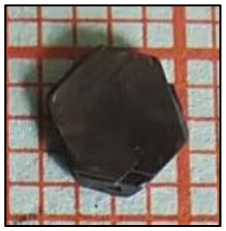
$CrTe_2$

Monolayer $WS_2$

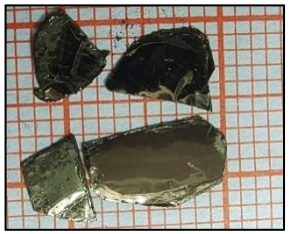
$HfTe_2$

Ferroelectric materials


$NbOI_2$

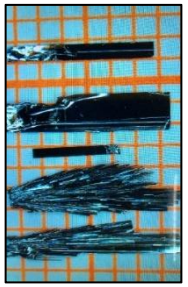
$NbOCl_2$


$NbOBr_2$

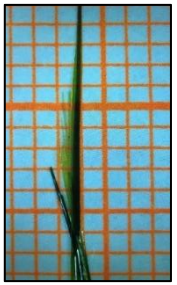
$VOCl_2$

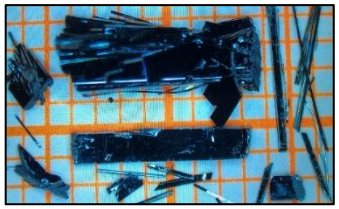
$TaOBr_2$

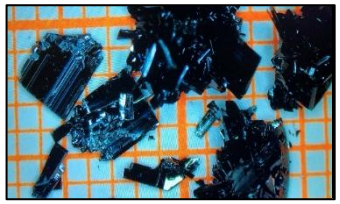
$TaOI_2$

# (4) Topological insulator

北京理工大學 BEIJING INSTITUTE OF TECHNOLOGY

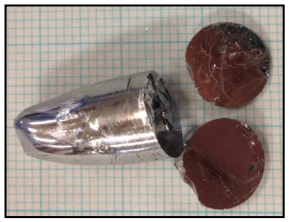

$Bi_2Se_3$

$Bi_2Te_3$

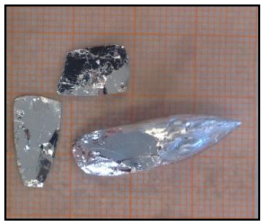

$Bi_{1.75}Sb_{0.25}Te_{1.85}Se_{1.15}$

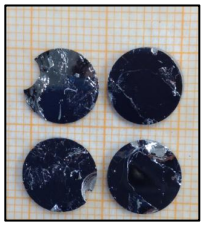

$Bi_{1.5}Sb_{0.5}Te_{1.7}Se_{1.3}$

$Bi_{1.25}Sb_{0.75}Te_{1.3}Se_{1.7}$

$BiSbTeSe_2$ ($BSTS_2$)

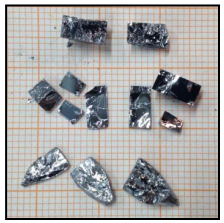

$BiSbTe_2S$

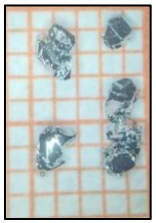

PbTe

$Sn_{0.03}$-$BSTS_2$

$Sn_{0.04}$-$BSTS_2$

$Sn_{0.05}$-$BSTS_2$

$In_{0.04}$-$BSTS_2$

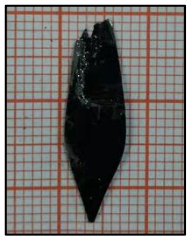

$In_{0.05}$-$BSTS_2$

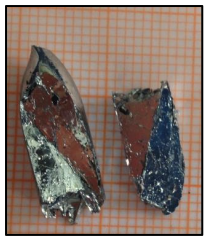

$Sr_{0.06}Sm_{0.1}Bi_{1.9}Se_3$

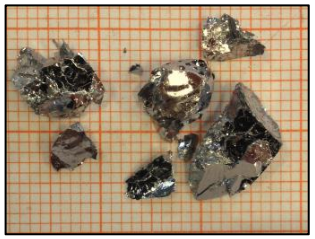

$Tl_{0.6}Bi_{1.9}Mn_{0.1}Te_3$

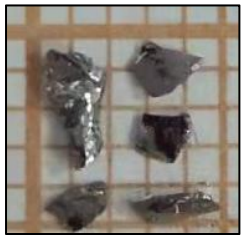

$Tl_4SnTe_3$

$Bi_4Br_4$

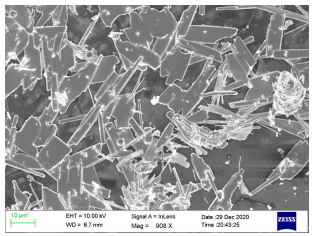

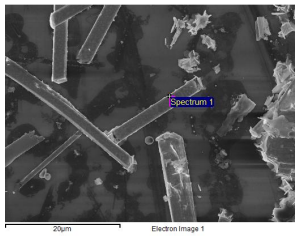


$Bi_4Br_4$ nanostructure

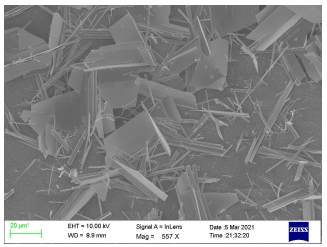

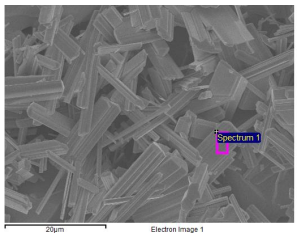


$Bi_4I_4$ nanostructure

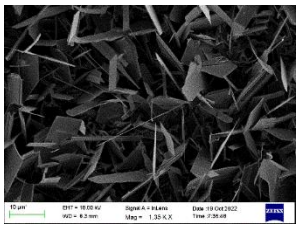

$Bi_2Se_3$ nanostructure

# (5) Topological semimetals

北京理工大學 BEIJING INSTITUTE OF TECHNOLOGY

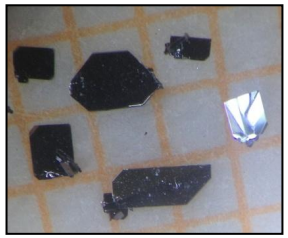
HfSiS

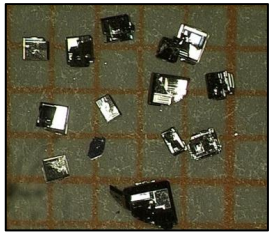
ZrSiSe

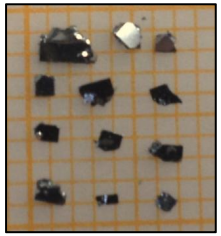
ZrGeS

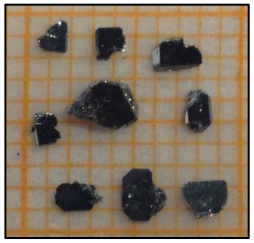
ZrGeSe

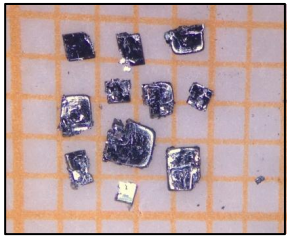
ZrGeTe

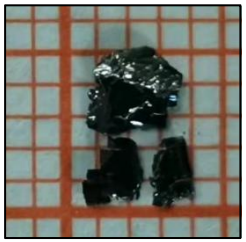
ZrSiS


$ZrTe_3$


NbP

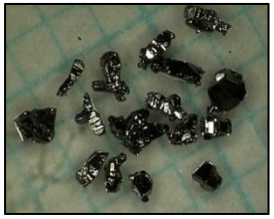
TaP

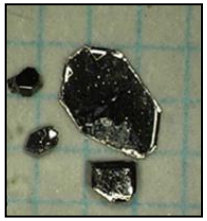
NbAs

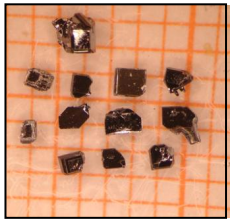
TaAs

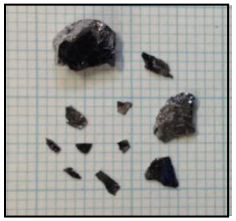
$SrSn_2As_2$


$SrIn_2As_2$


$(TaSe_4)_2I$


$T_d$-$WTe_2$


$Ta_3SiTe_6$


CoSi


KHgBi

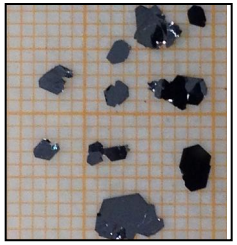
$TlTaSe_2$

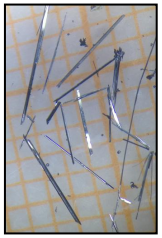
$HfTe_5$


$TaIrTe_4$

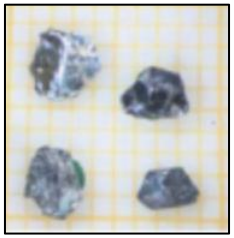
CaAuAs

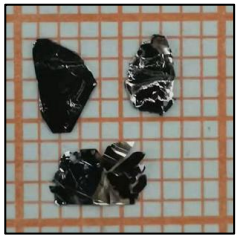
$NiTe_2$

# (6) Topological superconductor

北京理工大學 BEIJING INSTITUTE OF TECHNOLOGY

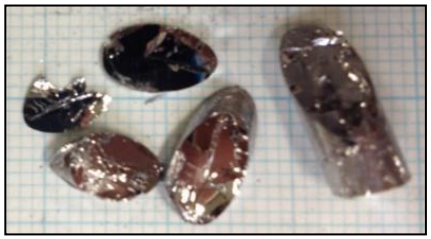

$Tl_{0.2}Bi_2Te_3$

$Tl_{0.3}Bi_2Te_3$

$Tl_{0.4}Bi_2Te_3$

$Tl_{0.5}Bi_2Te_3$

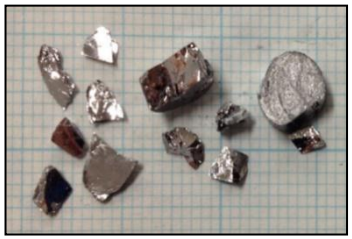

$Tl_{0.6}Bi_2Te_3$

$Tl_2Mo_6Se_6$

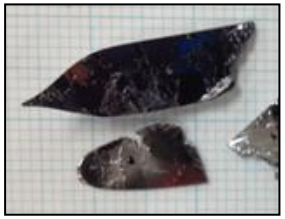

$Sr_{0.02}Bi_2Se_3$

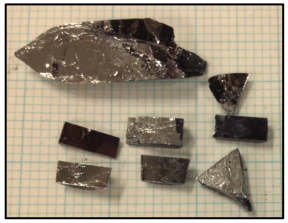

$Sr_{0.04}Bi_2Se_3$

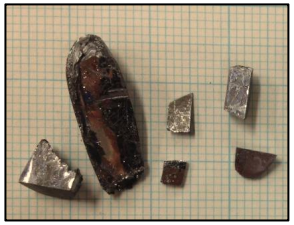

$Sr_{0.06}Bi_2Se_3$

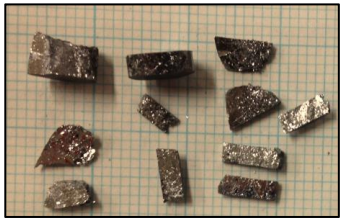

$Sr_{0.1}Bi_2Se_3$

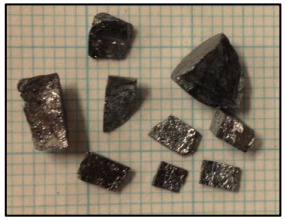

$Sr_{0.2}Bi_2Se_3$

$T_c$~ 4.2K

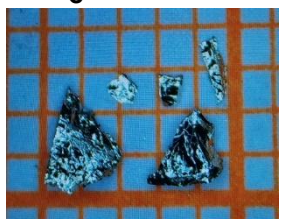

PdTe

$Cu_{0.3}Bi_2Se_3$

$Cu_{0.4}Bi_2Se_3$

$Cu_{0.5}Bi_2Se_3$

$Cu_{0.6}Bi_2Se_3$

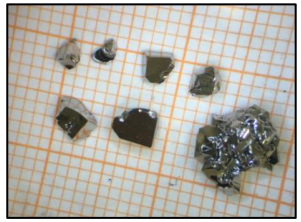

$In_{0.04}Sn_{0.96}Te$

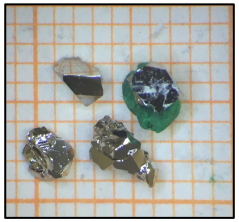

$In_{0.06}Sn_{0.94}Te$

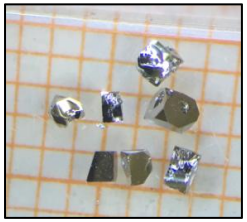

$In_{0.1}Sn_{0.9}Te$

# Outline

北京理工大學 BEIJING INSTITUTE OF TECHNOLOGY

- 1. Introduction of crystal and crystal growth
- 2. Crystal growth, physical properties of Kagome superconductors $AV_3Sb_5$
- 3. Exploration of topological superconductors
- 4. Summary

# Background

北京理工大學 BEIJING INSTITUTE OF TECHNOLOGY

## Electronic band structure of kagome materials

Coexistence of linear dispersion band and flat band in kagome material

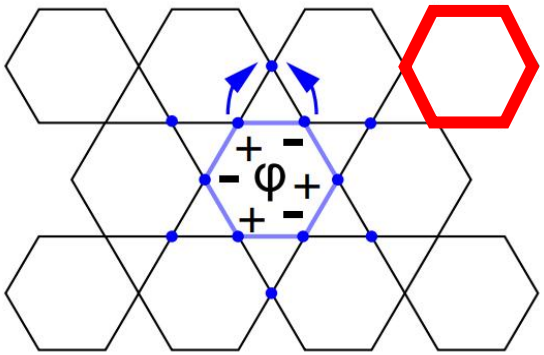


Localized electrons and honeycomb in the Kagome lattice

*Phys. Rev. Lett., 121.096401 (2018)*

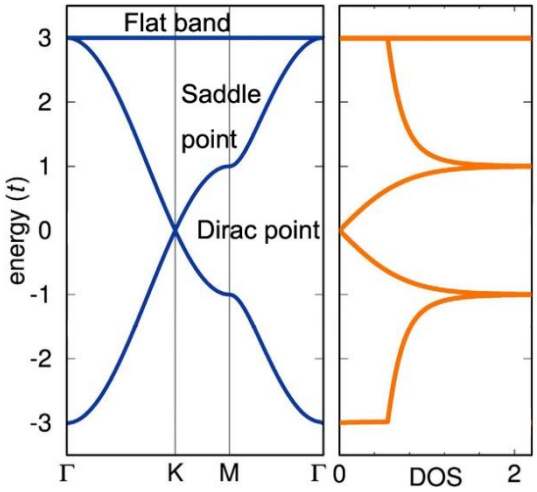


Band structure

Three features: Dirac point, Flat band, Saddle point

*Nat. Mater., 9. 163 (2020)*

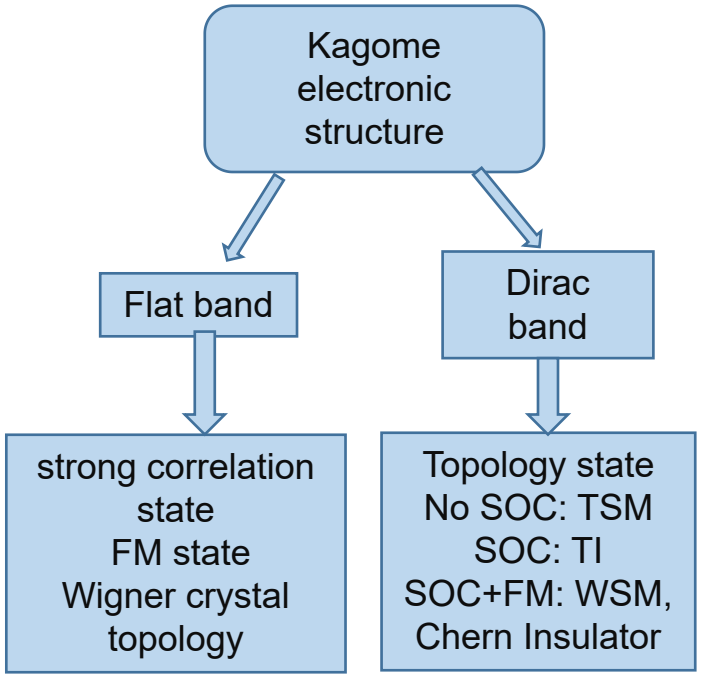

# Background

北京理工大學 BEIJING INSTITUTE OF TECHNOLOGY

## Superconductivity in $LaRu_3Si_2$ with Kagome structure

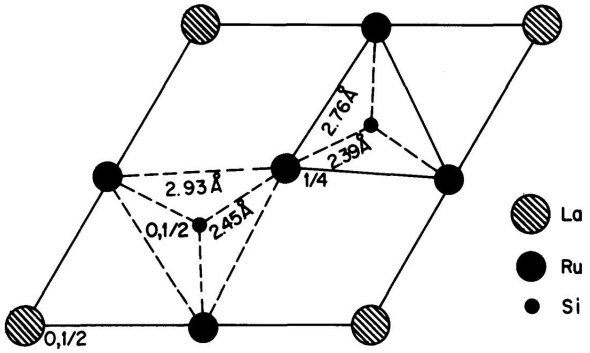


projection along [001] of the hexagonal phase $LaRu_3Si_2$.

Mat. Res. Bull., Vol. 15, pp. 1489–1491, 1980. Printed in the USA.
0025-5408/80/101489-03$02.00/0 

NEW TERNARY SUPERCONDUCTORS WITH SILICON

H. Barz
Bell Laboratories, Murray Hill, NJ 07974

(Received August 12, 1980; Communicated by B. Matthias)

ABSTRACT

A new superconducting ternary system with the formula $MRu_3Si_{2+x}$, where $x \sim +.2$ is reported. M is Y, La and Th. The superconducting transition temperatures range from 7.6 K for La to 3.5 K for Y.

# Discovery of $AV_3Sb_5$ (A = K, Rb, Cs) with Kagome lattice

北京理工大學 BEIJING INSTITUTE OF TECHNOLOGY

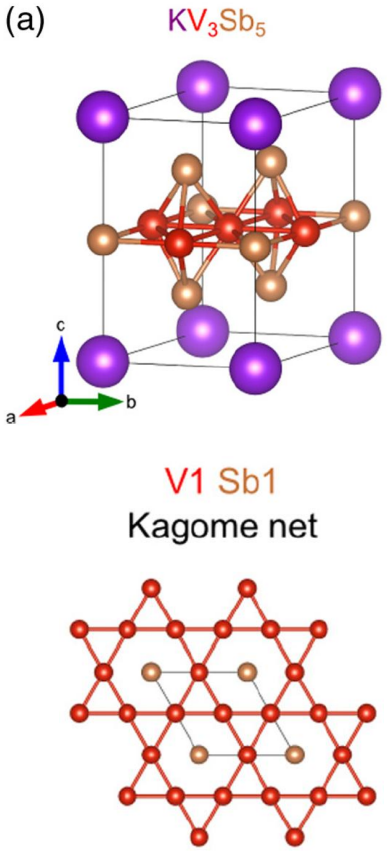


Crystal structure of $AV_3Sb_5$

B. R. Ortiz *et al*, *PRM*, **3**, 094407 (2019)

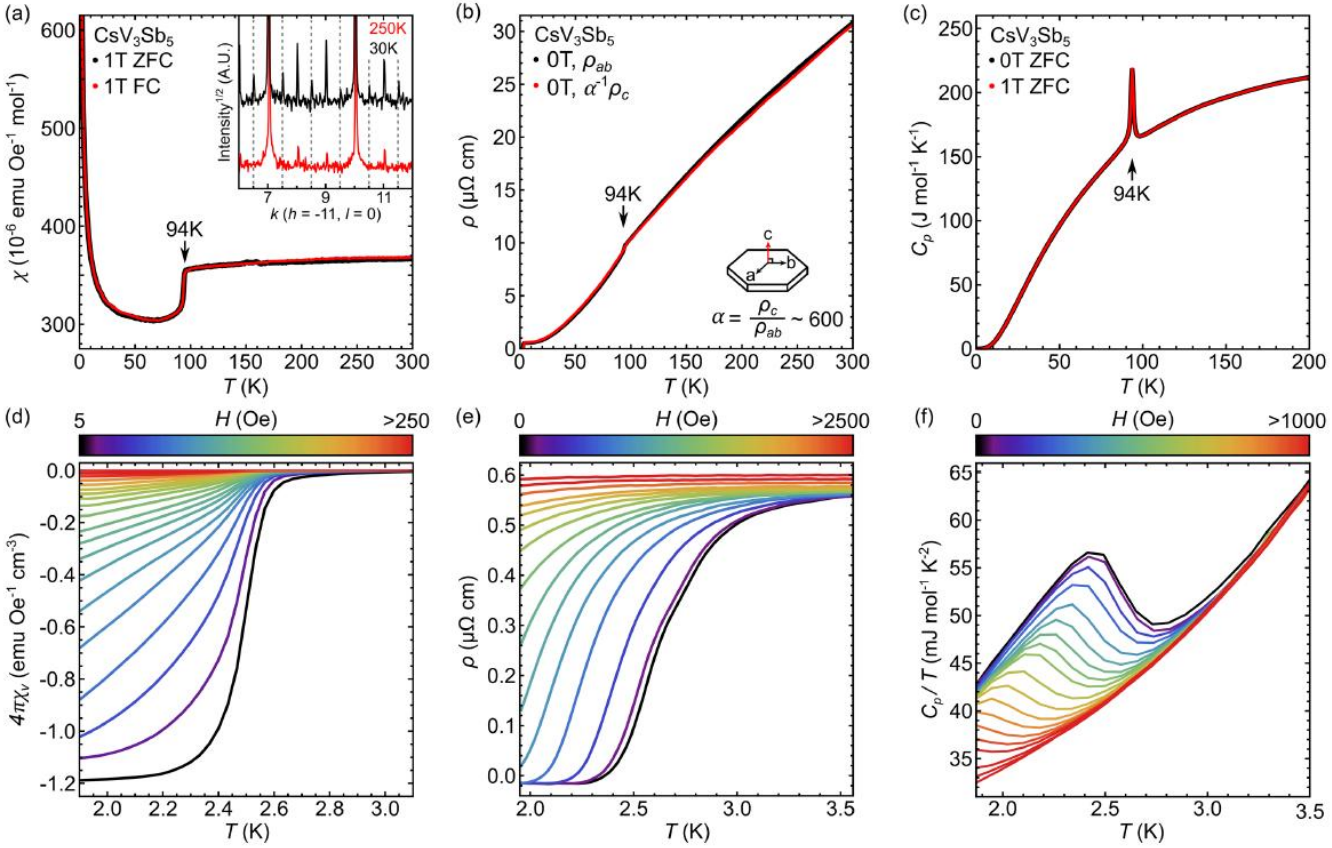


Magnetization, electrical resistivity, and heat capacity of $CsV_3Sb_5$

B. R. Ortiz *et al*, *PRL*, 125, 247002 (2020)

# Anomalous Hall effect and SdH oscillation of $KV_3Sb_5$

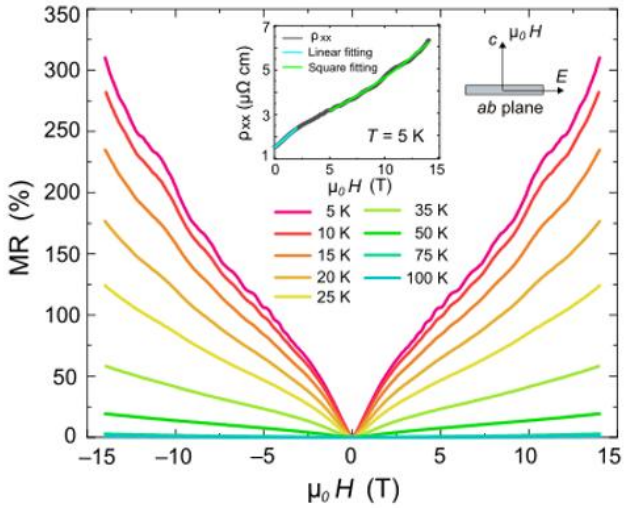


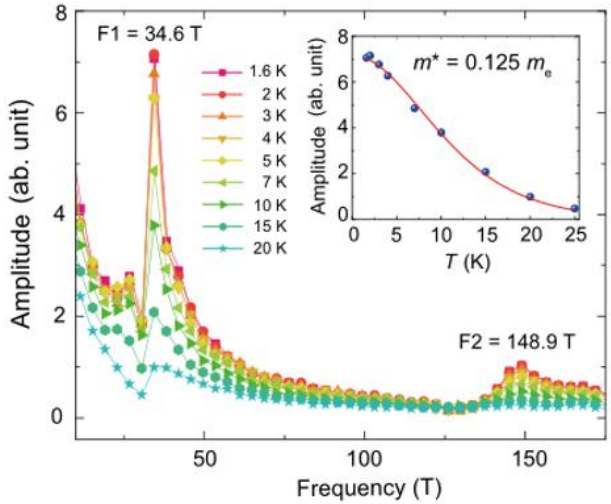


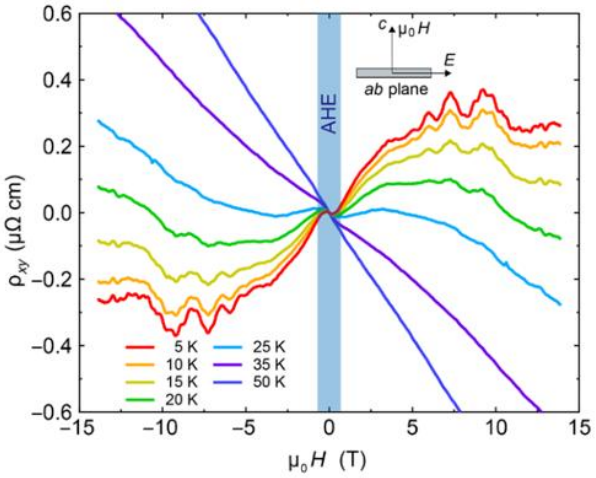


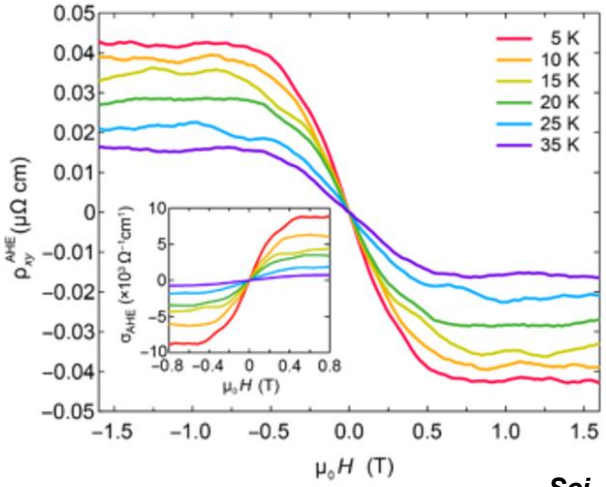


SdH oscillation and anomalous Hall effect of $KV_3Sb_5$

*Sci. Adv. 2020; 6 : eabb6003*

# Growth and Structure of Kagome materials $AV_3Sb_5$

北京理工大學 BEIJING INSTITUTE OF TECHNOLOGY

**Growth method:** flux method, ASb-Sb as flux

**Starting materials:** K (Rb, Cs), V, Sb

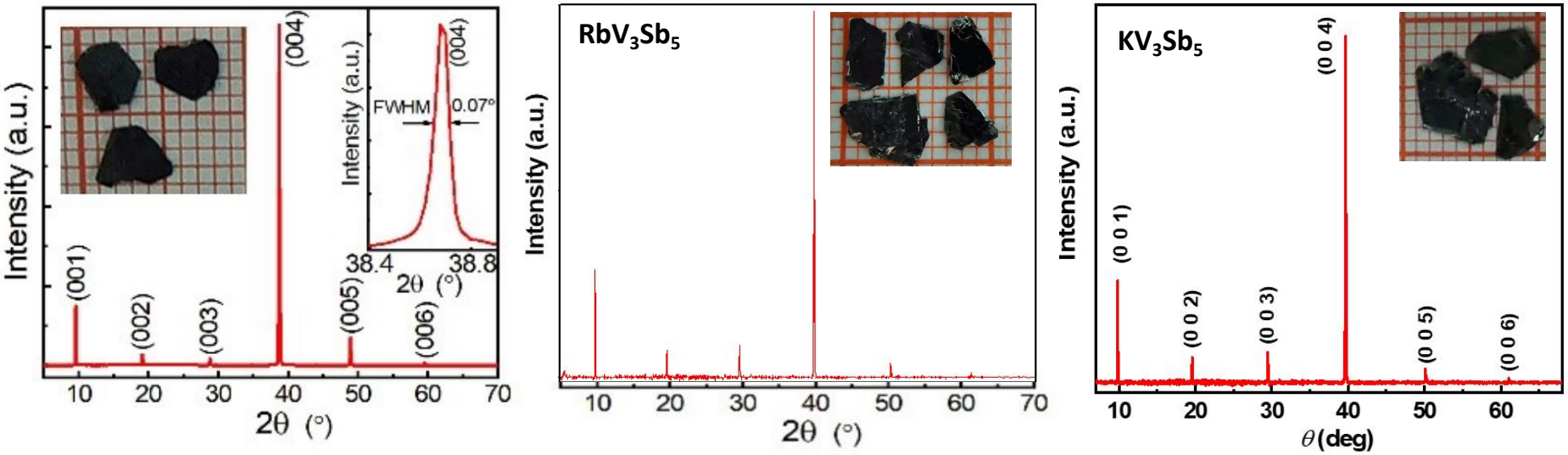


XRD patterns of $AV_3Sb_5$ single crystals

# Physical properties of $CsV_3Sb_5$

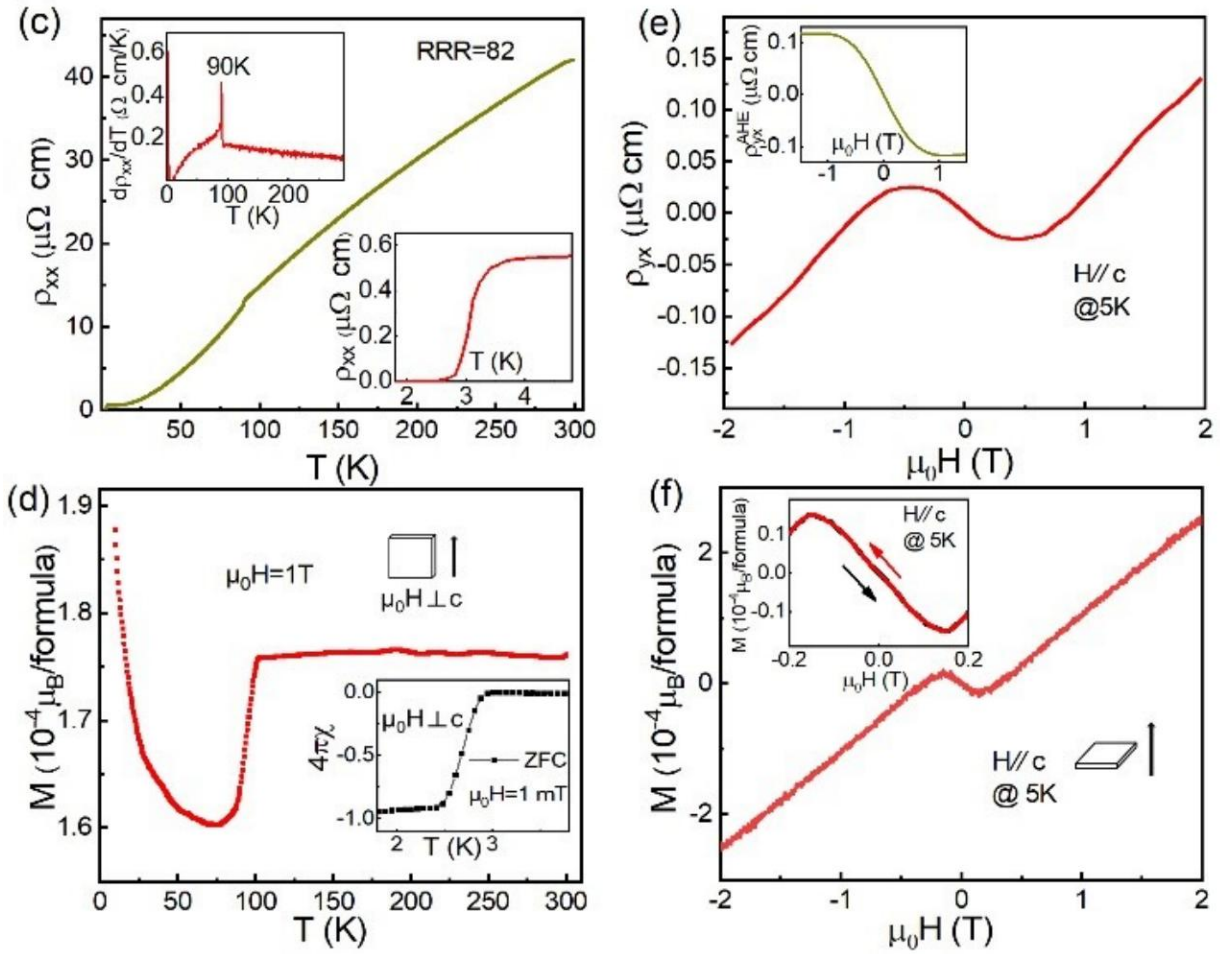


**(1) $T_{CDW}$~90K;**

**(2) $T_C$~3.2 K;**

**(3) AHE was observed.**

ZW Wang et al, PRB 104, 075148 (2021)

# Chiral charge order in $CsV_3Sb_5$

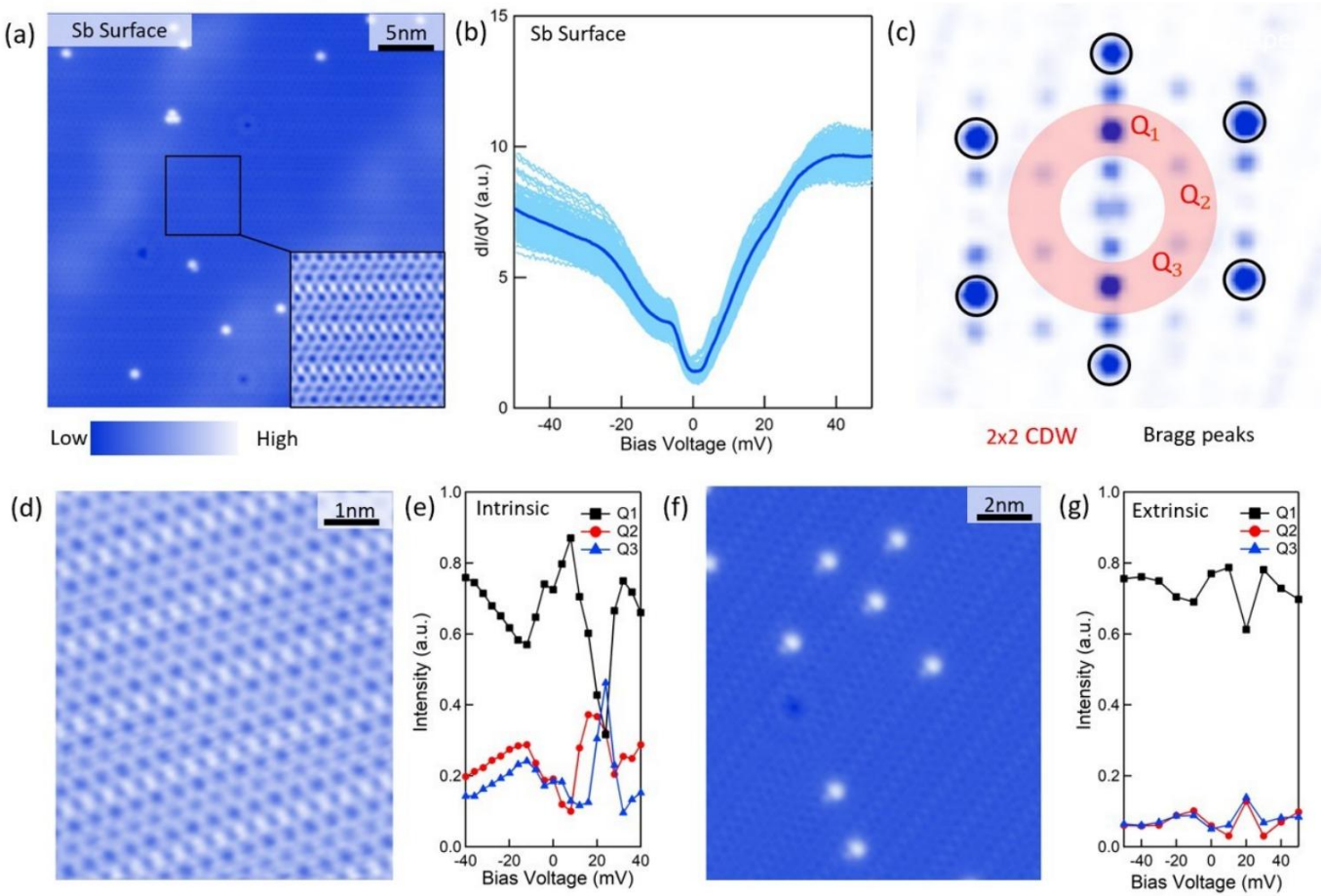


(1) charge order gap opening from -23meV to +35meV;

(2) 2X2 charge order, red shaded area;

(3) 1X4 charge order along Q1;

(4) Chiral charge order,

ZW Wang et al, PRB 104, 075148 (2021)

# Superconducting tunneling spectrum of $CsV_3Sb_5$

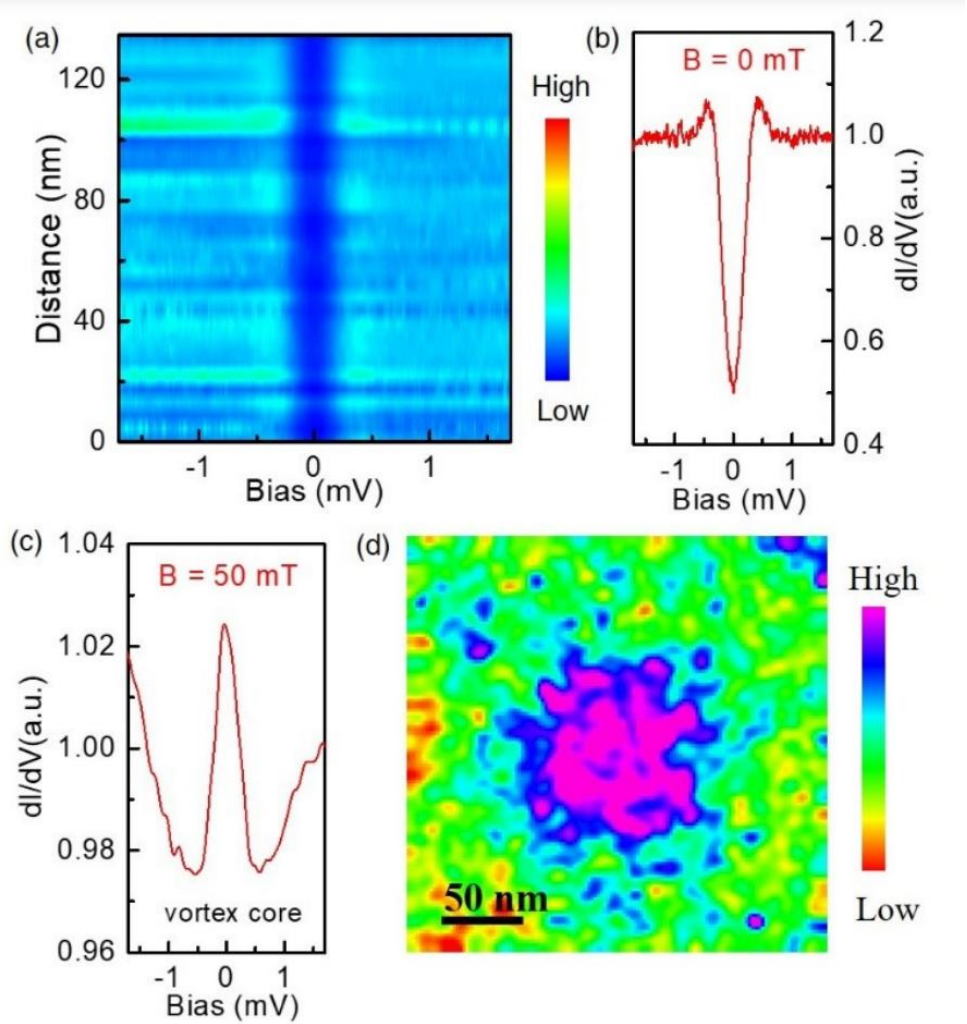


(1) the tunneling spectrums show an energy gap with a gap size $2\Delta$=0.85meV; the SC coupling strength $2\Delta/k_BT_C$=3.9, which is slightly larger than the standard BCS value and suggests the electron pairing is close to a moderate coupling.

(2) a zero-energy vortex core state was observed with applying a 50mT magnetic field along the c-axis

ZW Wang et al, PRB 104, 075148 (2021)

# Nematic Superconductivity in $CsV_3Sb_5$

北京理工大學 BEIJING INSTITUTE OF TECHNOLOGY

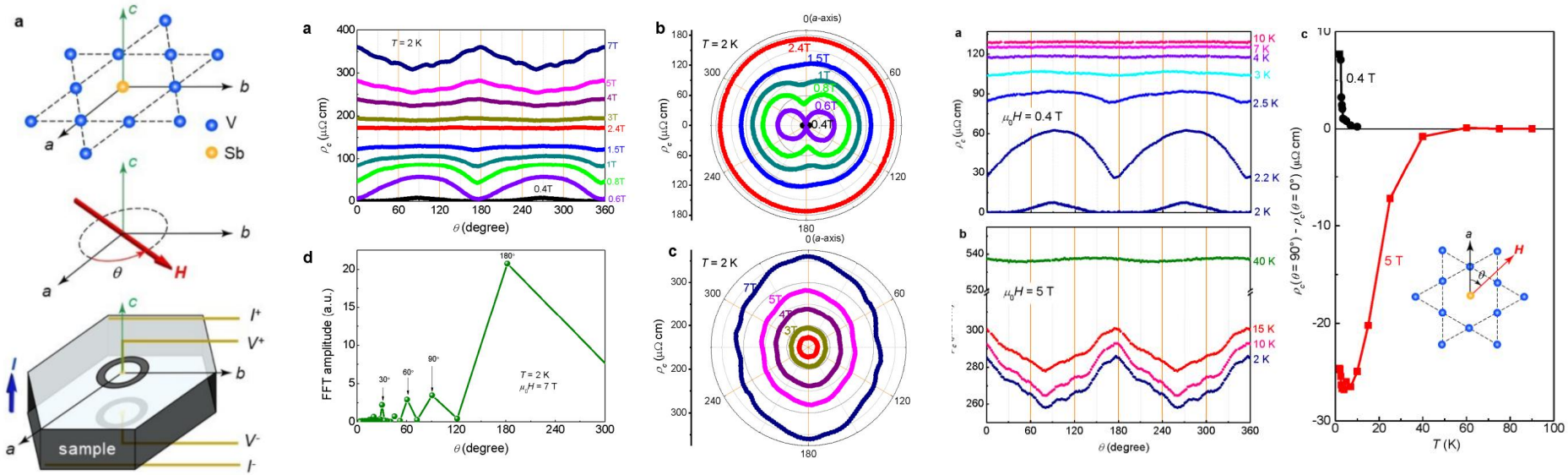


Twofold symmetry of angular dependent c-axis resistivity under in-plane magnetic field

Temperature evolution of the nematicity of c-axis resistivity

Y. Xiang, **ZW Wang**, H.-H. Wen, *et al,* Nat. Commun. 12, 6727 (2021)

# Band structure of $CsV_3Sb_5$ revealed by ARPES

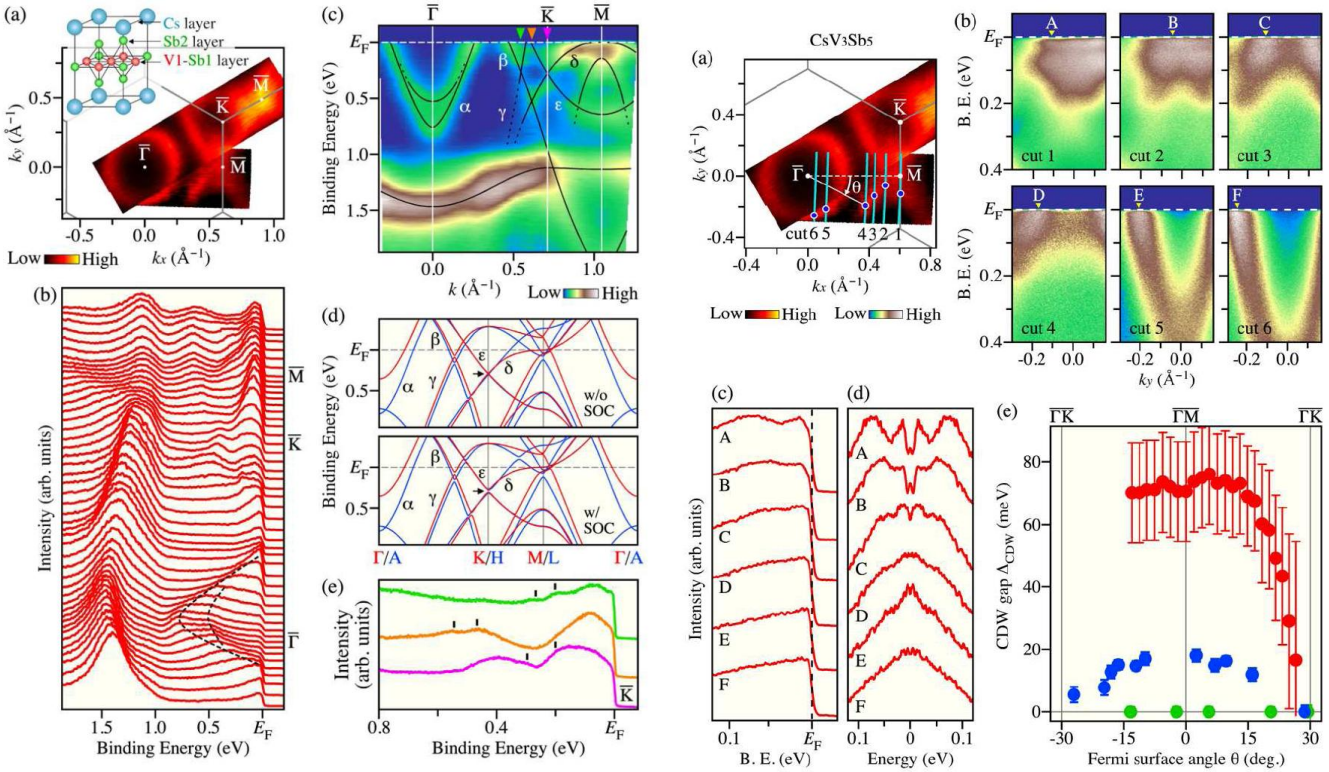


- the energy gap on the multiple Dirac points due to the SOC;
- different types of CDW gap, the larger CDW gap for the saddle point around the M point, the smaller CDW gap for the Dirac band, and the absence of CDW gap for the electron band at Γ. The CDW gap also displays a strong anisotropy.

K. Nakayama, **ZW Wang**, T. Sato et al, *PRB* 104, L161112 (2021)

# Manipulating the band structure of $CsV_3Sb_5$ by Cs dosing

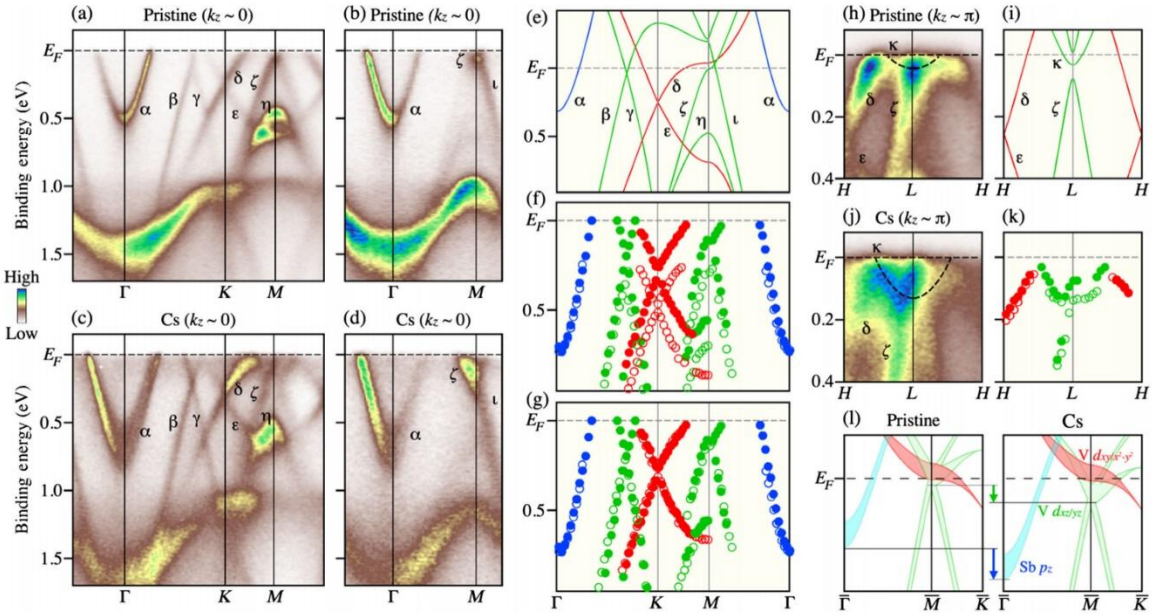


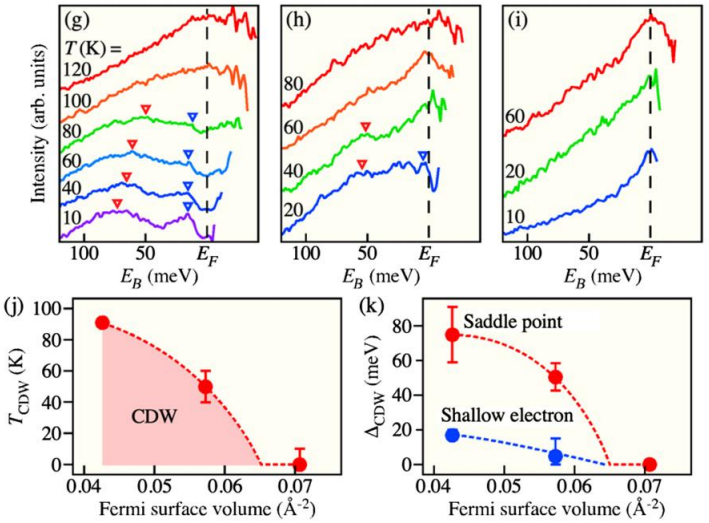


- electron doping to $CsV_3Sb_5$ by Cs dosing proceeds in an orbital-selective way;
- a marked increase in electron filling of the Sb $5_{pz}$ and V$3d_{xz/yz}$ bands; while decrease of the V $3d_{xy/x2-y2}$ bands;
- CDW can be completely killed by Cs dosing while keeping the saddle point with the V $3d_{xy/x2-y2}$ character almost pinned at the Fermi level

K. Nakayama, **ZW Wang**, T. Sato et al, *PRX* 12, 011001 (2022)

# Manipulating SC and CDW in $CsV_3Sb_5$ by chemical doping

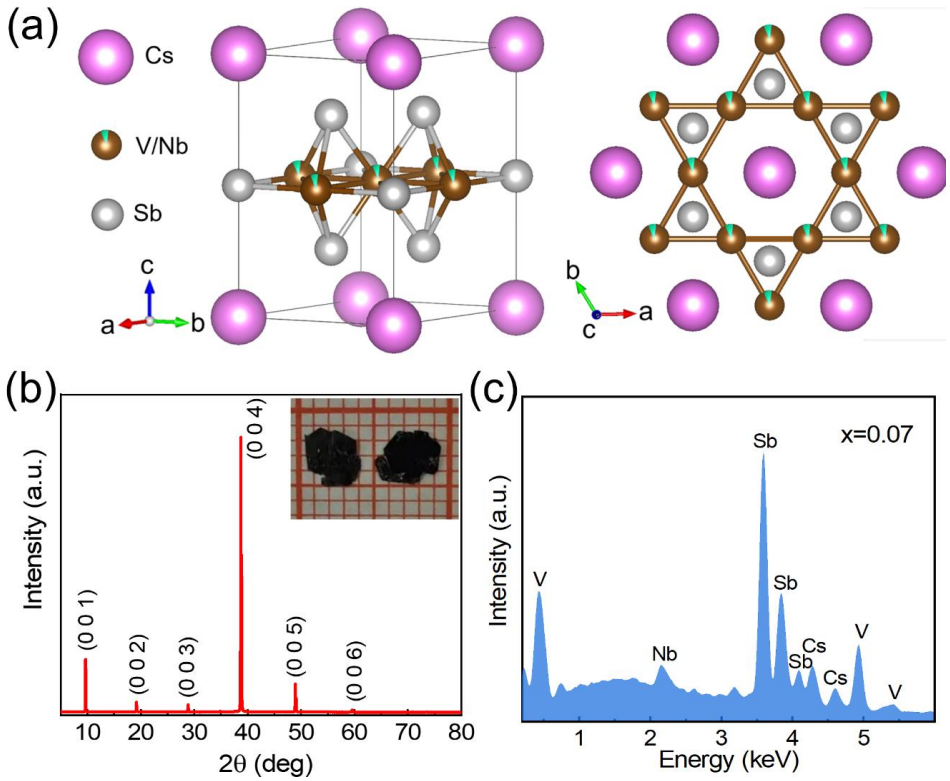


Crystal structure and chemical composition of $Cs(V_{1-x}Nb_x)_3Sb_5$.

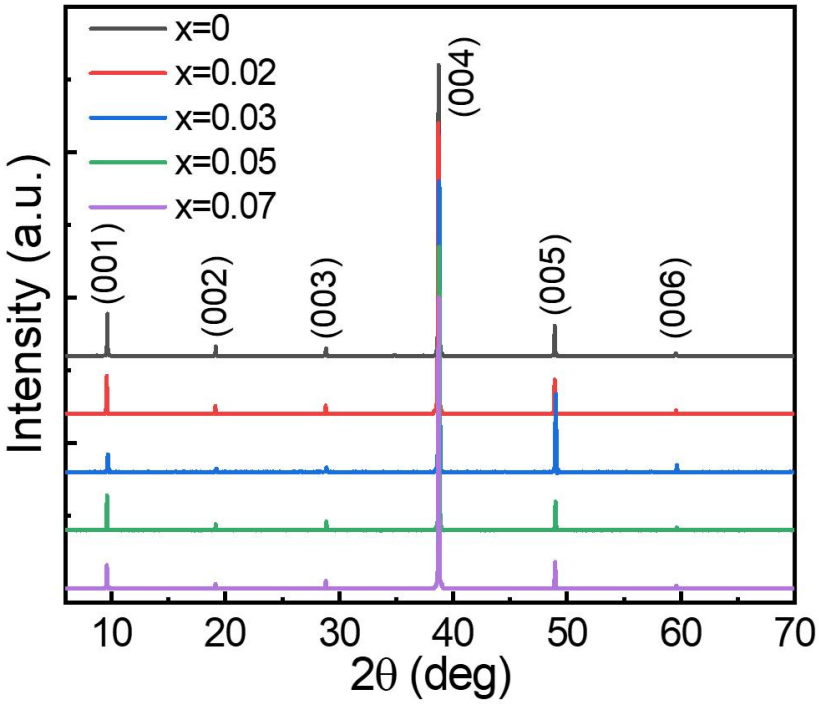


XRD patterns for $Cs(V_{1-x}Nb_x)_3Sb_5$ single crystals

YK Li, **ZW Wang** *et al*, Phys. Rev. B 105, L180507 (2022)

# Competition of CDW and SC in Nb-doped $CsV_3Sb_5$

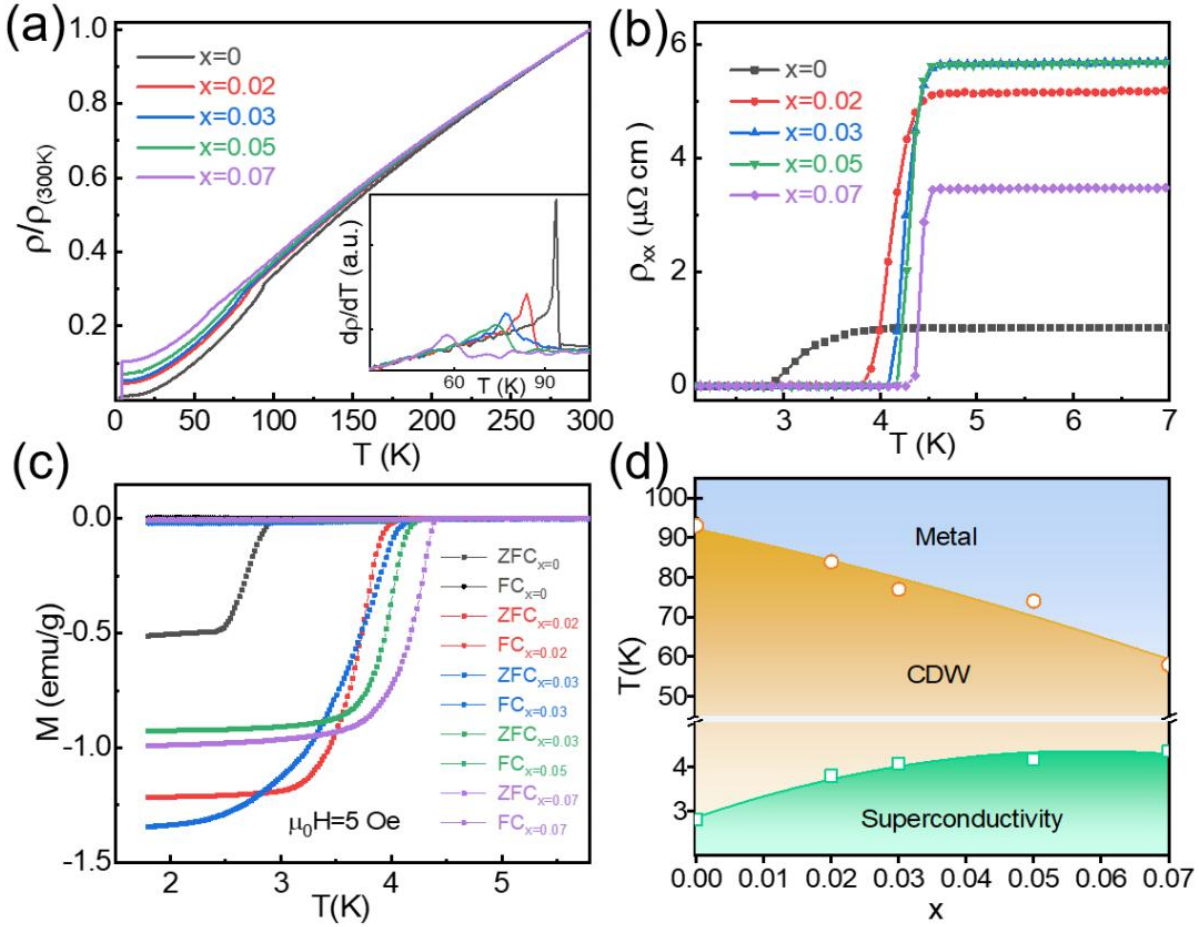


Temperature dependence of resistivity and magnetization of Nb-$CsV_3Sb_5$

- Nb doping induces apparent suppression of CDW order and promotes superconductivity;
- Competition between SC and CDW;

YK Li, **ZW Wang** *et al*, Phys. Rev. B 105, L180507 (2022)

# AHE in Nb-doped $CsV_3Sb_5$

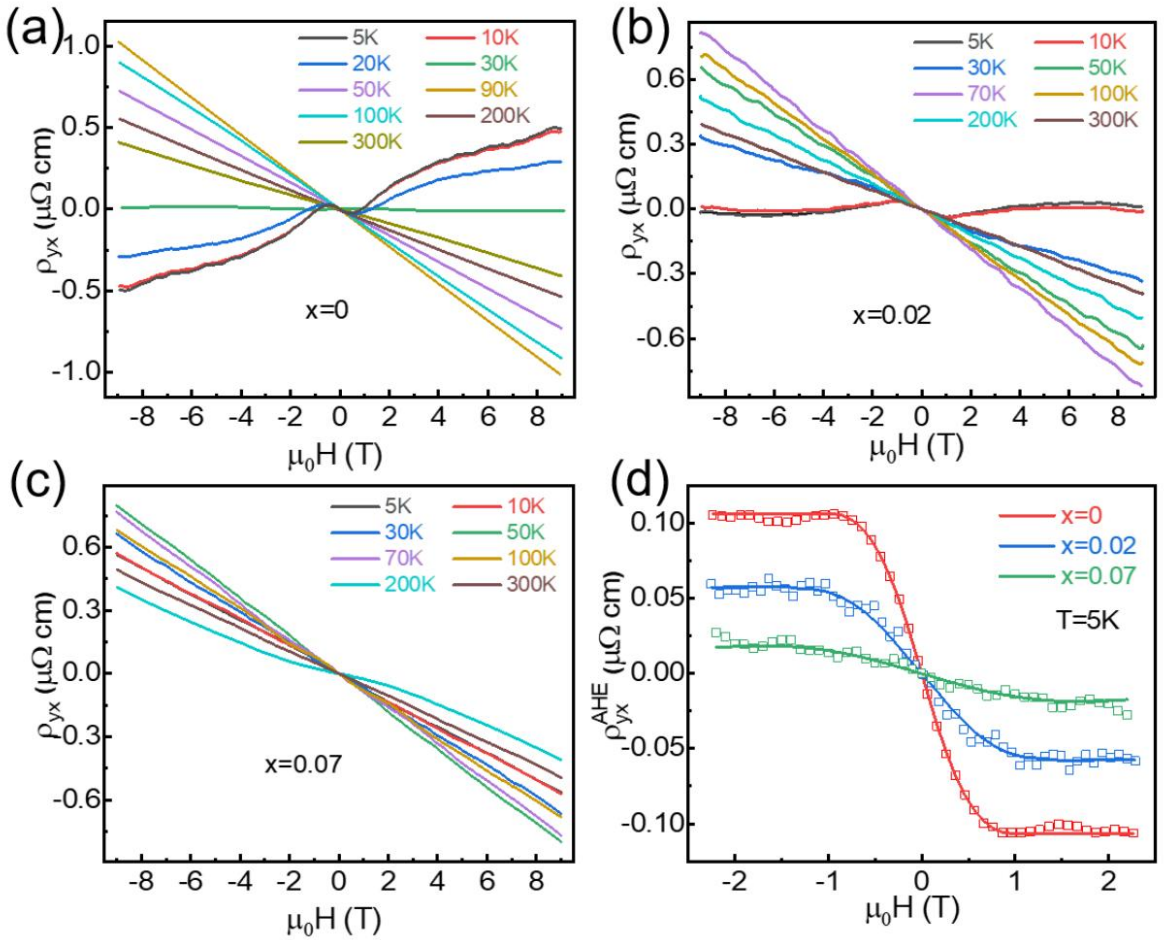


- AHE becomes weaker and weaker with Nb doping in $CsV_3Sb_5$, together with the suppression of CDW;
- hall resistivity displays linear behavior at high temperature;
- multiband dominated at low temperature, transfer to single band dominated at high temperature.

YK Li, **ZW Wang** *et al*, Phys. Rev. B 105, L180507 (2022)

# Magnetoresistance in Nb-doped $CsV_3Sb_5$

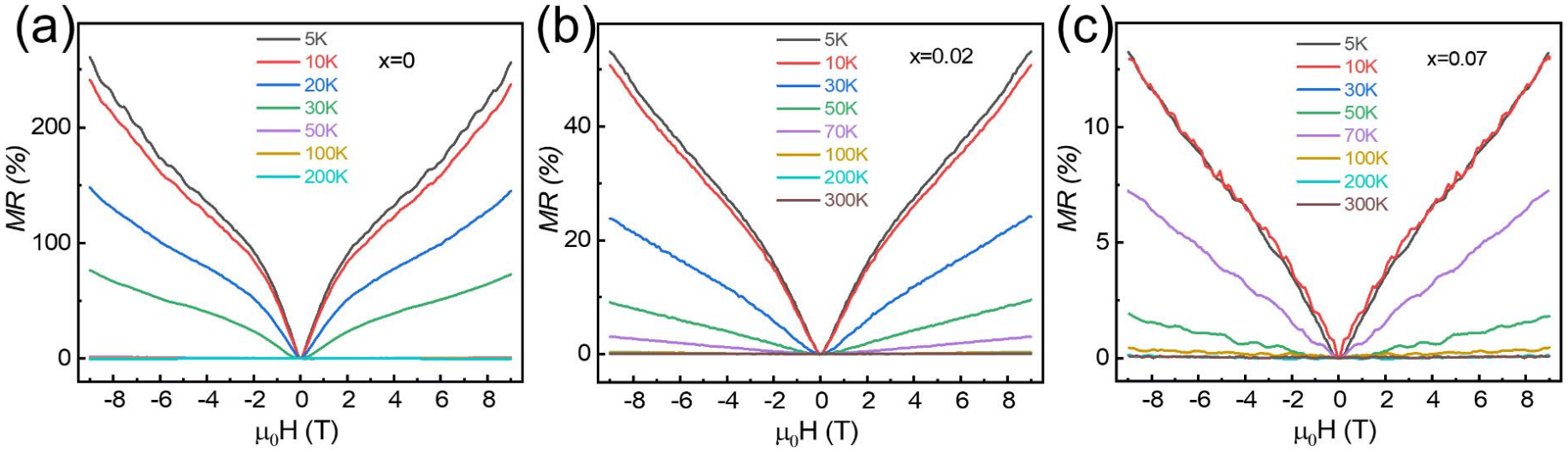


MR becomes weaker and weaker with Nb doping in $CsV_3Sb_5$, together with the suppression of CDW

YK Li, **ZW Wang** *et al*, Phys. Rev. B 105, L180507 (2022)

# Band structure of Nb-doped $CsV_3Sb_5$

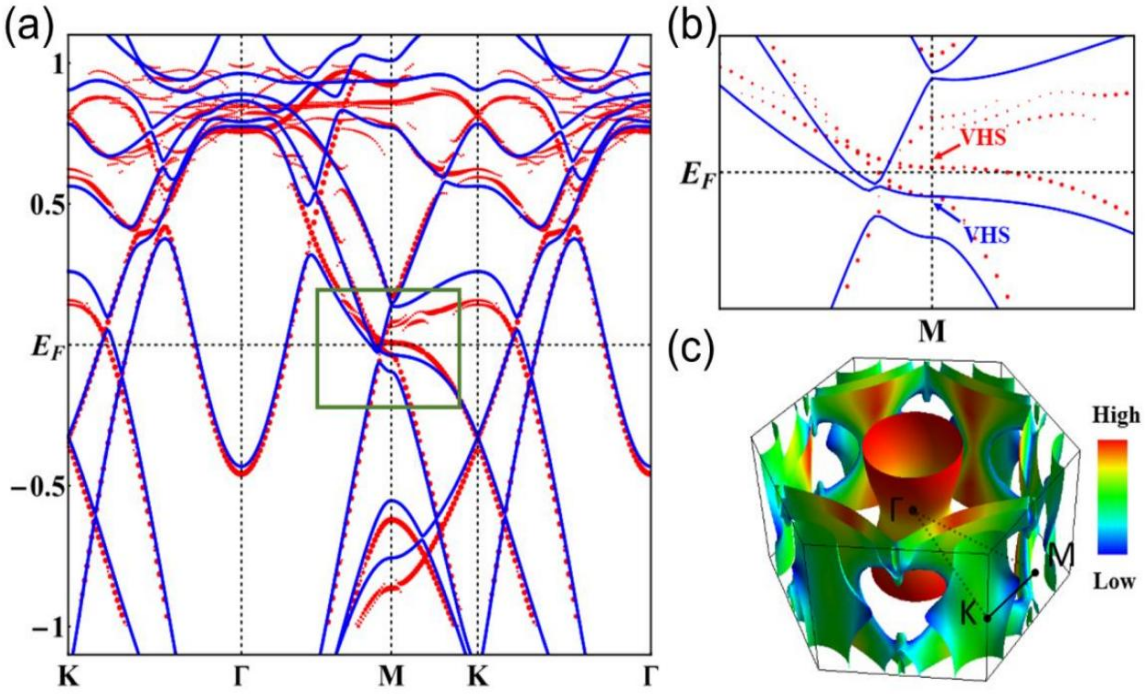


Electronic structures of $Cs(V_{1-x}Nb_x)_3Sb_5$ (x = 0.07)

- in the undoped sample, the saddle point (van Hove singularity, VHS) at M point is slightly below the Fermi energy, by Nb doping, this VHS band moves up and crosses the Fermi energy;
- modify the Fermi surface giving rise to a broken hole on the Fermi surface in the path between Γ and M point. Thus depletes the filled DOS of VHS near M, and weaken the instability of the saddle points, leading to the suppression of CDW.
- the Fermi energy is lifted a little bit near Γ, enlarge the electron like Fermi surface around Γ.

YK Li, **ZW Wang** *et al*, Phys. Rev. B 105, L180507 (2022)

# Observed band structure of Nb-doped $CsV_3Sb_5$

北京理工大學 BEIJING INSTITUTE OF TECHNOLOGY

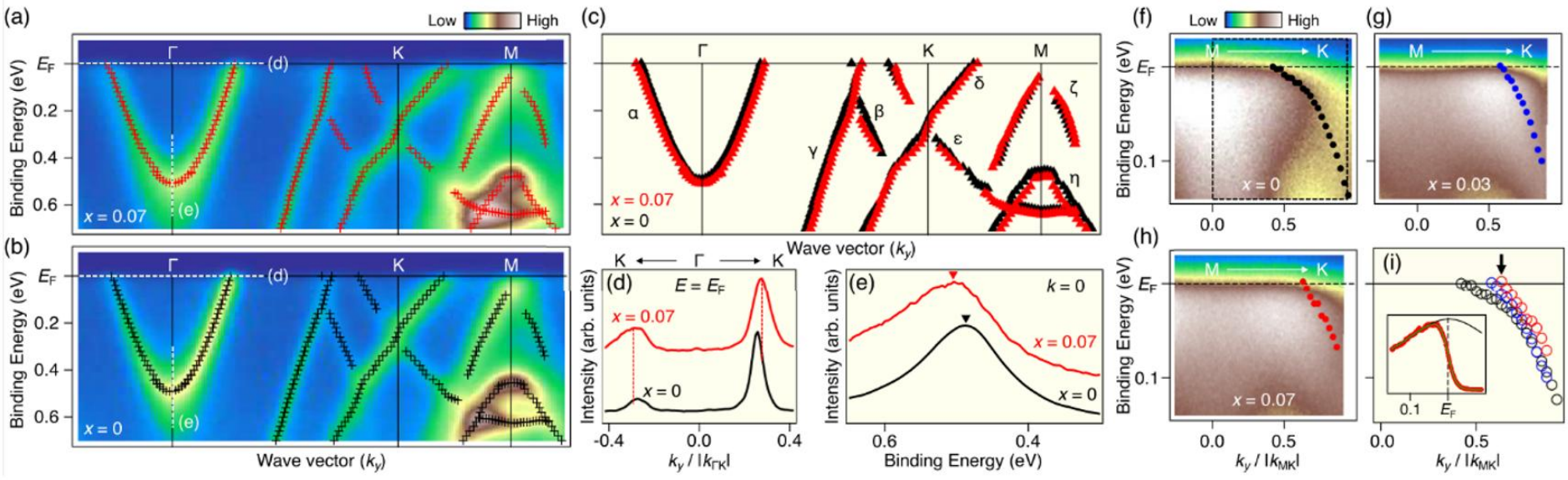


Band structure of pristine and Nb-doepd CVS revealed by ARPES at 120K

- Nb substitution shifts the Sb-derived electron band at the Γ point downward, enlarge the electron pocket near $E_F$, enhance SC;
- moves the V-derived band around the M point upward, lift up the saddle point (SP) away from the Fermi level, leading to the reduction of the CDW-gap magnitude and $T_{CDW}$.

T Kato, **ZW Wang**, T Sato, et al, PRL, 129, 206402 (2022)

# Crystal structure of Ta-doped $CsV_3Sb_5$

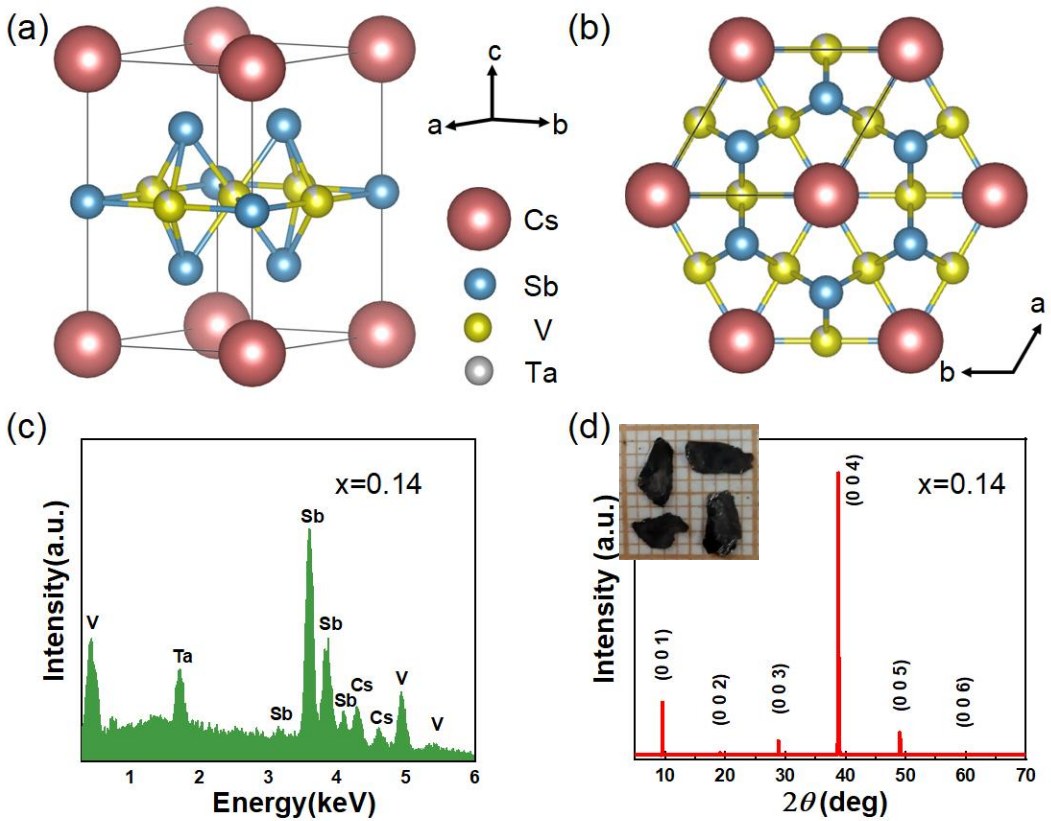


Crystal structure and chemical composition of $Cs(V_{1-x}Ta_x)_3Sb_5$.

Structure information of $Cs(V_{1-x}Ta_x)_3Sb_5$

| | |
|---|---|
| Empirical formula | $Cs(V_{0.86}Ta_{0.14})_3Sb_5$ |
| Formula weight(g/mol) | 949.44 |
| Temperature | 293 K |
| Crystal system | hexagonal |
| Space group | P 6/m m m |
| Unit cell dimensions | |
| a(Å) | 5.5587(12) |
| b(Å) | 5.5587(12) |
| c(Å) | 9.302(3) |
| α | 90° |
| β | 90° |
| γ | 120° |
| Volume(Å$^3$) | 248.92(13) |
| Z | 1 |
| Density (g/cm$^3$) | 6.334 |
| Absorption coefficient(mm$^{-1}$) | 23.801 |
| F(000) | 400 |
| $R_1$, $wR_2$ | 0.0577; 0.1660 |

| | x/a | y/b | z/c | U(eq) |
|---|---|---|---|---|
| Sb1 | 0.666667 | 0.333333 | 0.25561(11) | 0.0218(8) |
| Sb2 | 0.0 | 0.0 | 0.5 | 0.0208(8) |
| V1 | 0.5 | 0.5 | 0.5 | 0.0179(9) |
| Ta1 | 0.5 | 0.5 | 0.5 | 0.0179(9) |
| Cs1 | 0.0 | 0.0 | 0.0 | 0.0364(9) |

Atomic coordinates and equivalent isotropic displacement parameters

# TEM characterization of Ta-doped $CsV_3Sb_5$



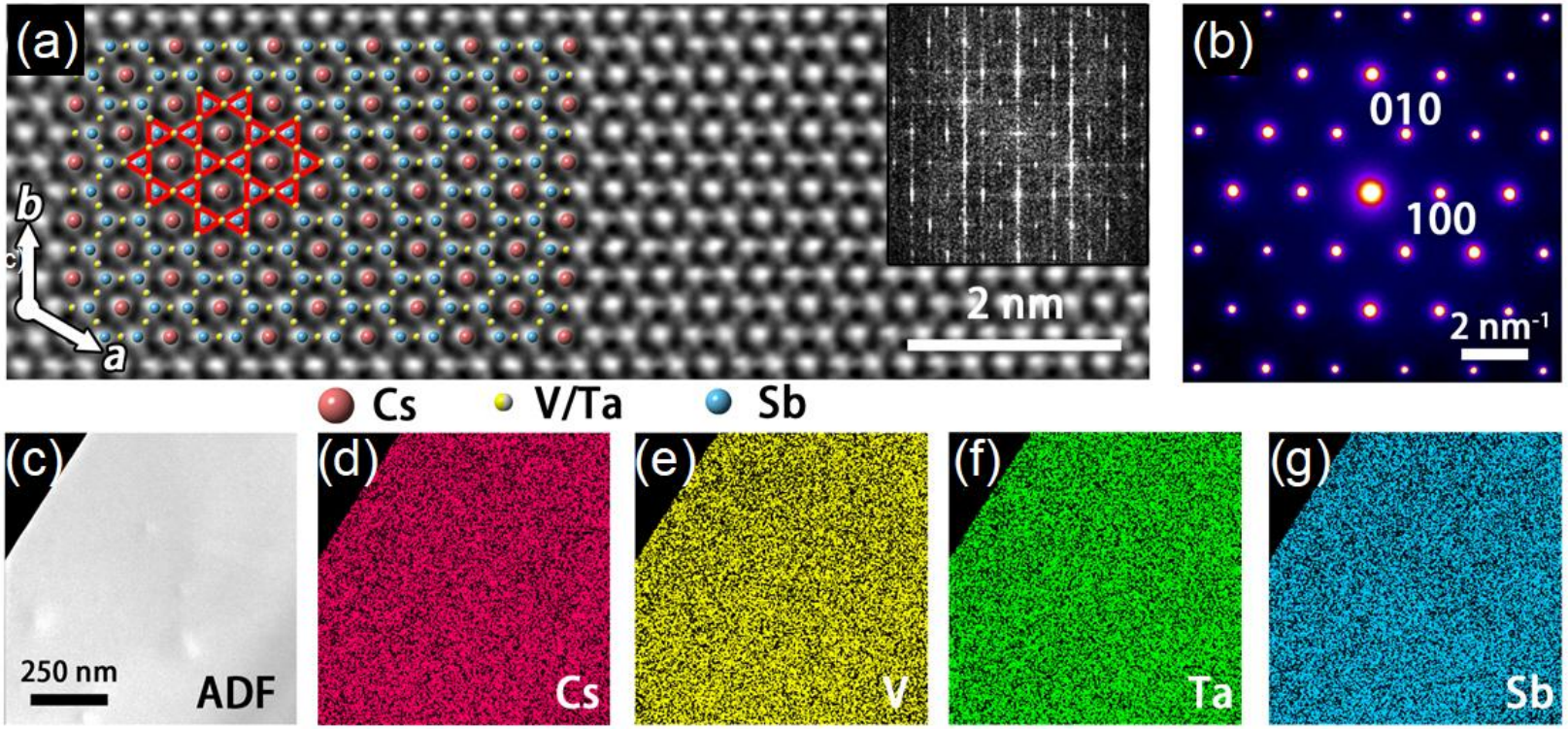


Structural characterization and element distribution of $Cs(V_{0.84}Ta_{0.16})_3Sb_5$

- Ta distributed homogenously in Ta-doped $CsV_3Sb_5$

# Competition of CDW and SC in Ta-doped $CsV_3Sb_5$

北京理工大學 BEIJING INSTITUTE OF TECHNOLOGY

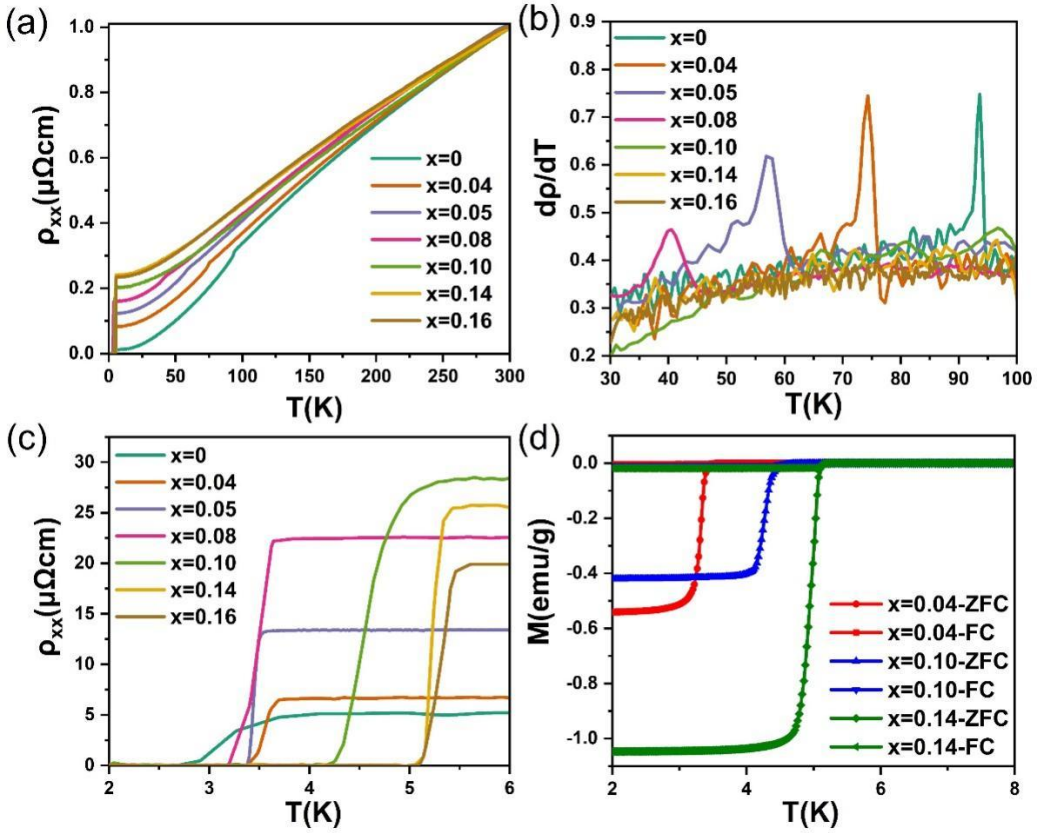


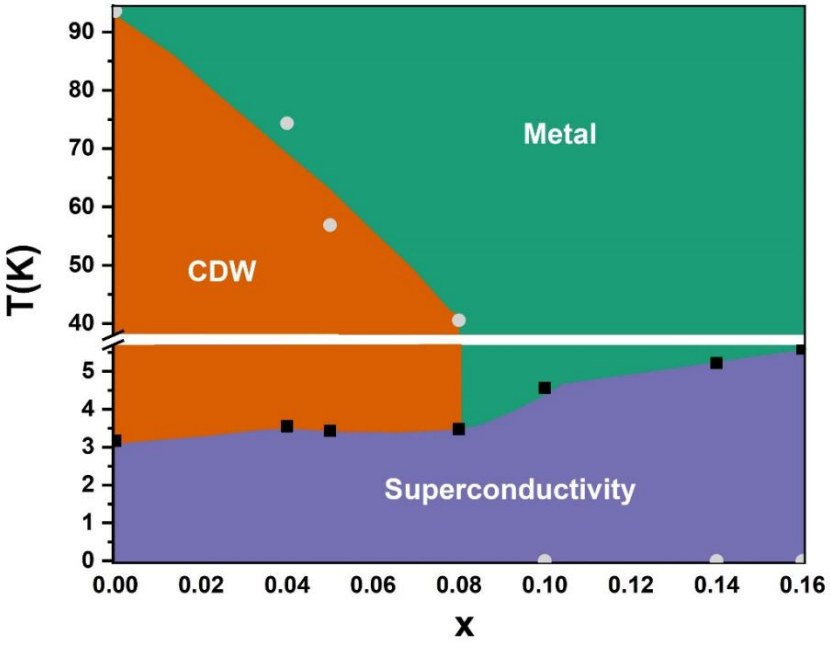


Phase diagram of Ta-$CsV_3Sb_5$

Temperature dependence of resistivity and magnetization of Ta-$CsV_3Sb_5$

Jinjin Liu et al, will be submitted

# Nodeless electron pairing in $CsV_3Sb_5$-derived Kagome superconductors

北京理工大學 BEIJING INSTITUTE OF TECHNOLOGY

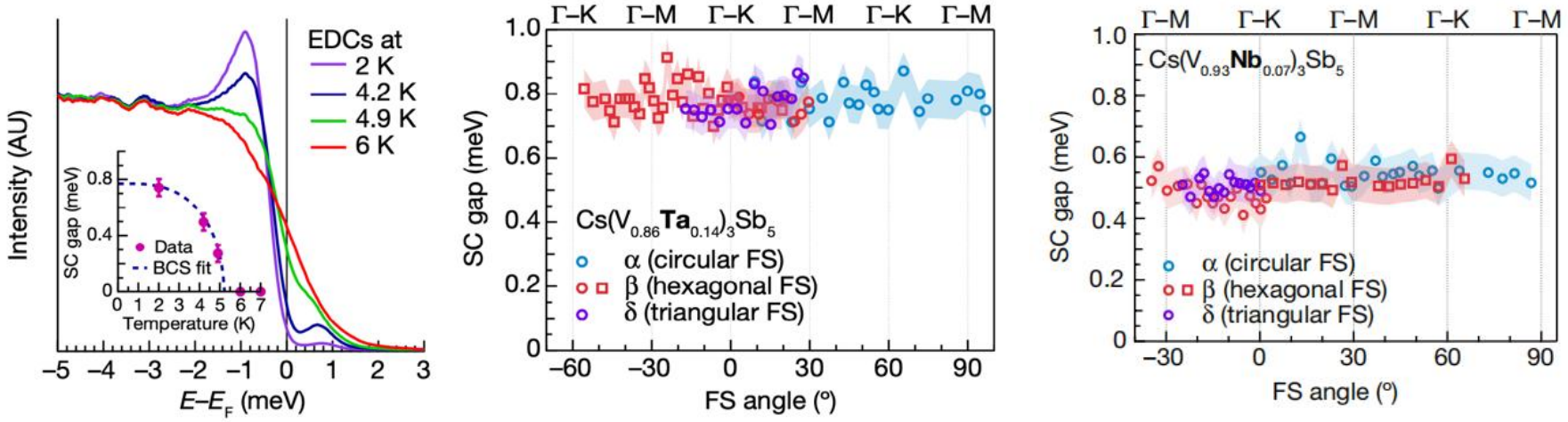


EDCs and momentum dependent SC gap of $Cs(V_{0.86}Ta_{0.14})_3Sb_5$ and $Cs(V_{0.93}Nb_{0.07})_3Sb_5$

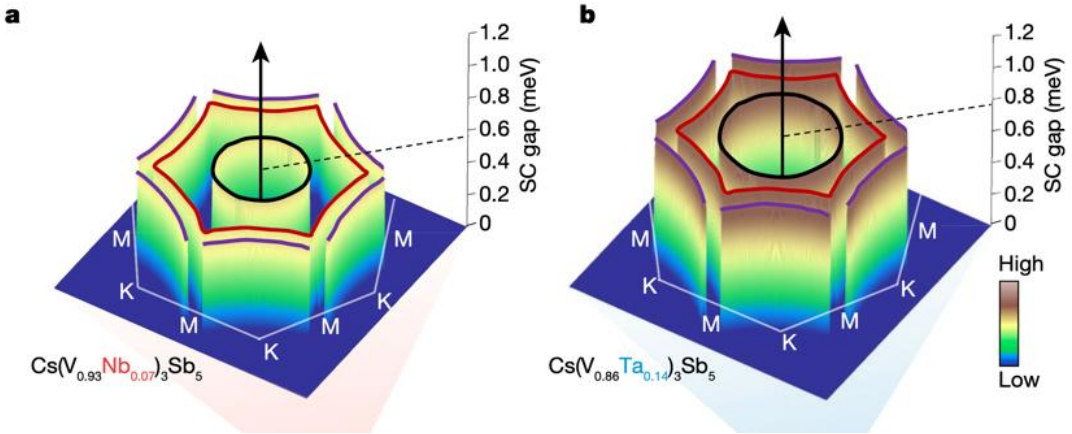


- a nodeless, nearly isotropic superconducting gap;
- The gap structure is robust to the appearance or absence of CDW.

Robust nodeless paring in $CsV_3Sb_5$systems

Y Zhong, **ZW Wang**, K Okazaki, et al, Nature (2023) online

# Outline

北京理工大學 BEIJING INSTITUTE OF TECHNOLOGY

- 1. Introduction of crystal and crystal growth
- 2. Crystal growth, physical properties of Kagome superconductors $AV_3Sb_5$
- 3. Exploration of topological superconductors
- 4. Summary

3. Exploration of topological superconductors

a) doping based on topological insulator

b) applied external pressure based on topological materials

# 3. Exploration of topological superconductors

a) doping based on topological insulator

b) applied external pressure based on topological materials

# Background

北京理工大學 BEIJING INSTITUTE OF TECHNOLOGY

## Topological superconductors (TSC)

- Topological superconductors: gapped in the bulk, with topologically protected gapless surface Andreev bound states.

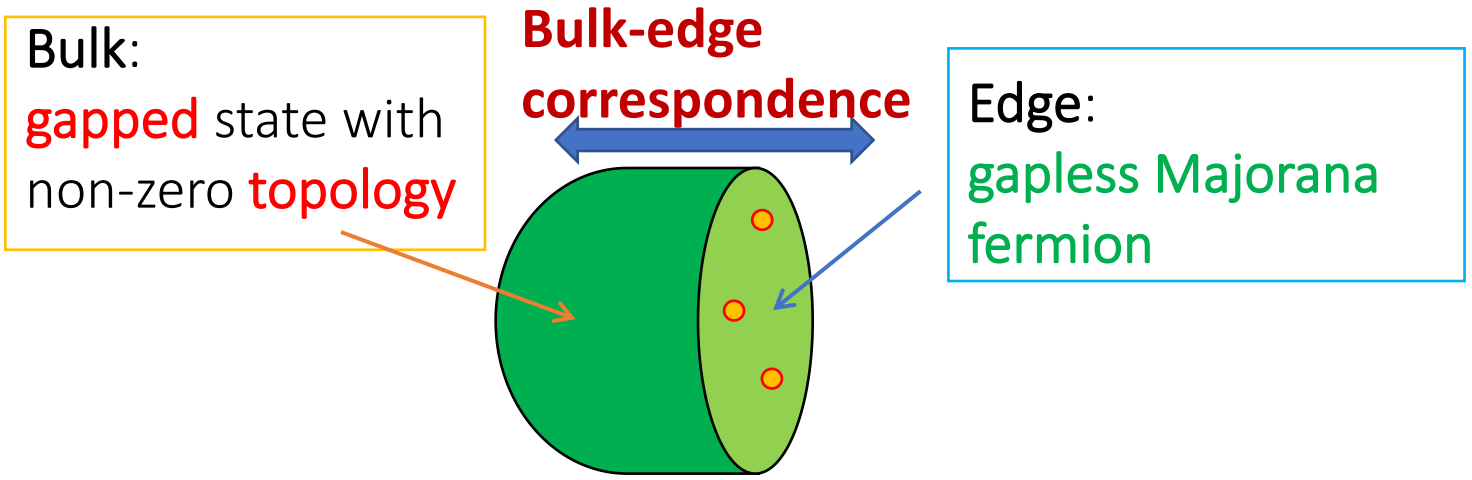


- Majorana fermions: Particles are their own antiparticles.

- TSC has great potential applications in fault-tolerant topological quantum computing.

# Background

Two ways to make TSCs:

(1) superconducting proximity effect based devices;

(2) doping or high-pressure based on topological materials.

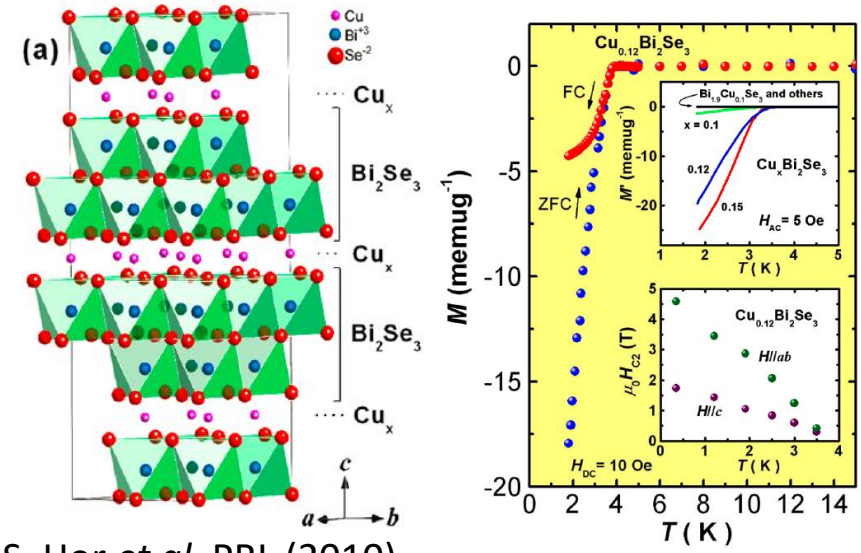


Y. S. Hor *et al*, PRL (2010)

Superconductivity in $Cu_xBi_2Se_3$

melting method, low SC volume fraction (20%)

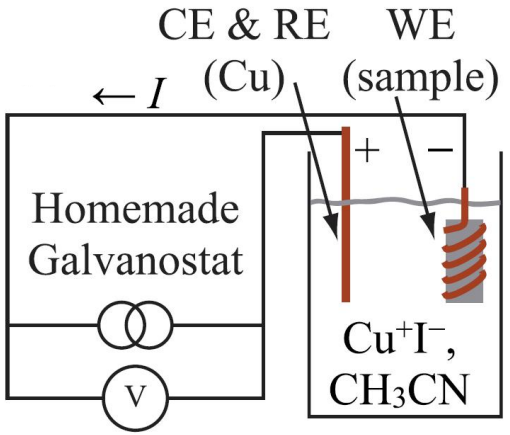


M. Kriener *et al*, PRB (2011)

Superconducting $Cu_xBi_2Se_3$ grown by electrochemistry method

higher volume fraction (up to 70%)

unstable in air, unable to develop a device

# Growth of $Tl_xBi_2Te_3$

北京理工大學 BEIJING INSTITUTE OF TECHNOLOGY

Using melting method,

Elemental shots of Tl (4N), Bi (6N) and Te (6N) are sealed in a quartz tube with nominal composition $Tl_xBi_2Te_3$ (x=0.1-0.8), then put into a furnace and heat at 750 °C for 50 h, following cool down to 550 °C in 100 h and then quenched in ice-water.

sealed tubes

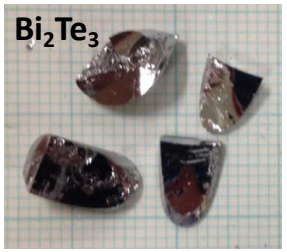


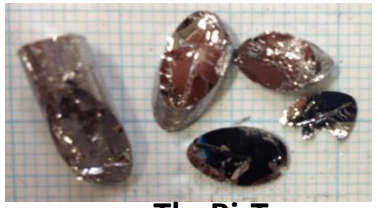


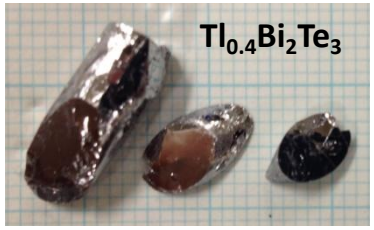



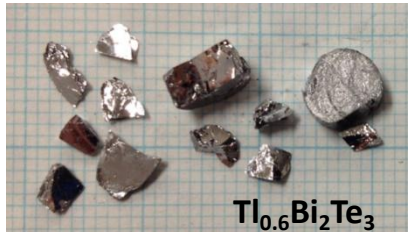


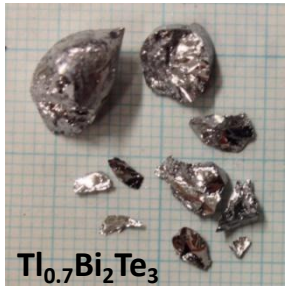


images of crystals

$x \leq 0.6$, good crystals, easy to cleave

x=0.7, small crystal, not easy to cleave

$x \geq 0.8$, no single crystal

# Structure of $Tl_xBi_2Te_3$

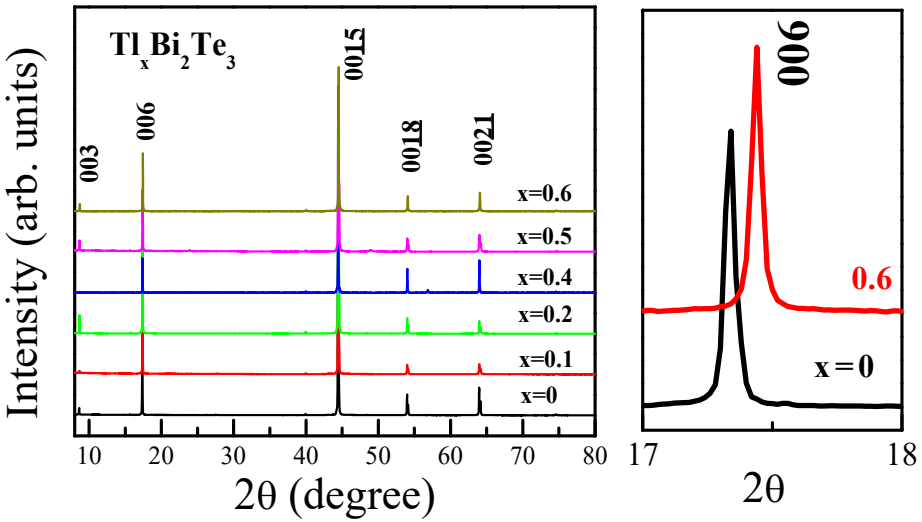


Single crystal XRD patterns of $Tl_xBi_2Te_3$

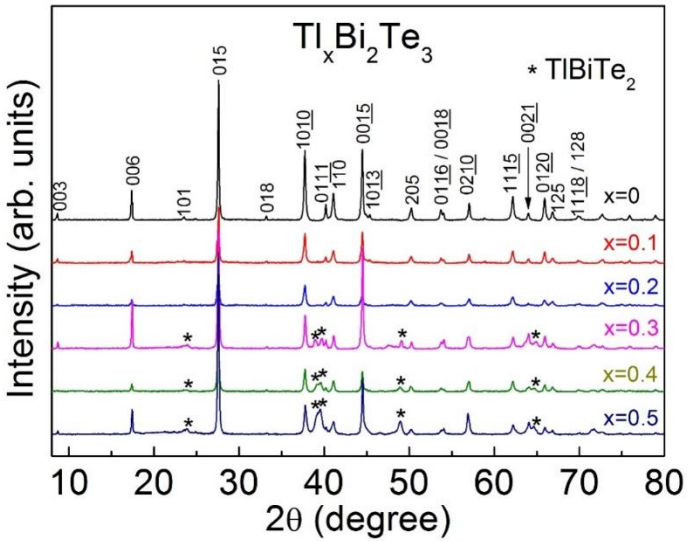


Powder XRD patterns of $Tl_xBi_2Te_3$

after Tl doping, main structure didn't change;
c-axis becomes shorter;
impurity phase of $TlBiTe_2$ appears in powder XRD data for x larger than 0.2
because of the instability of the superconducting phase, it is possible that the $TlBiTe_2$ impurity phase occurs upon grinding

# Rietveld refinement of $Tl_{0.6}Bi_2Te_3$

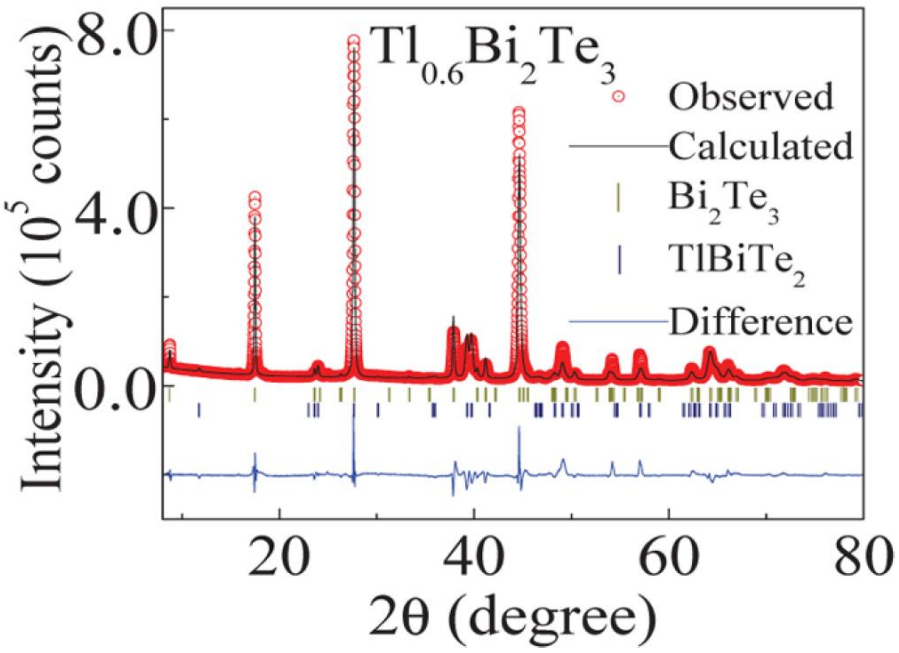


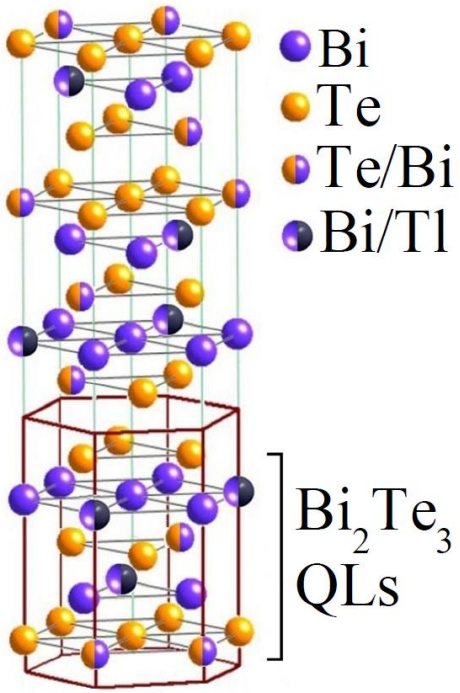


neither intercalation of Tl, nor interstitial of Tl;
a large mount of Bi vacancy (1/3);
$Bi_{Te}$ antisite defect

Z. Wang *et al*, *Chem. Mater.* (2016)

# ICP results of $Tl_xBi_2Te_3$

北京理工大學 BEIJING INSTITUTE OF TECHNOLOGY

| $x$ | Nominal composition | Tl | Bi | Te |
|---|---|---|---|---|
| 0.1 | $Tl_{0.1}Bi_2Te_3$ | 0.106(1) | 2.087(6) | 3 |
| 0.2 | $Tl_{0.2}Bi_2Te_3$ | 0.207(2) | 2.098(6) | 3 |
| 0.3 | $Tl_{0.3}Bi_2Te_3$ | 0.233(2) | 2.090(6) | 3 |
| 0.4 | $Tl_{0.4}Bi_2Te_3$ | 0.396(4) | 2.077(6) | 3 |
| 0.5 | $Tl_{0.5}Bi_2Te_3$ | 0.526(5) | 2.040(6) | 3 |
| 0.6 | $Tl_{0.6}Bi_2Te_3$ | 0.609(6) | 2.059(6) | 3 |

Molar ratio of Tl, Bi, and Te in the single crystal samples of TlxBi2Te3

# Magnetic properties of $Tl_xBi_2Te_3$

北京理工大學 BEIJING INSTITUTE OF TECHNOLOGY

SC volume fraction at 1.75 K

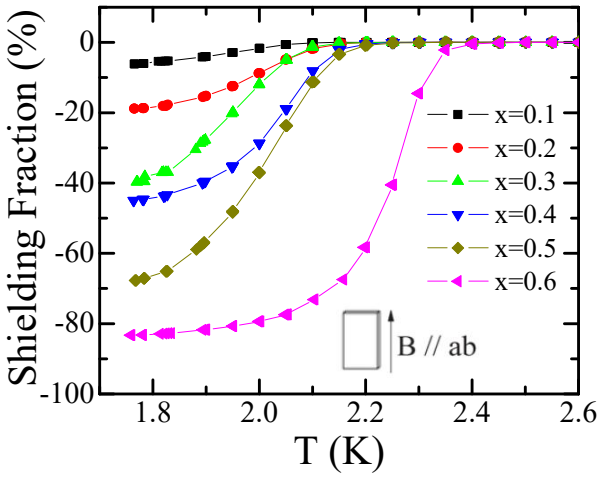


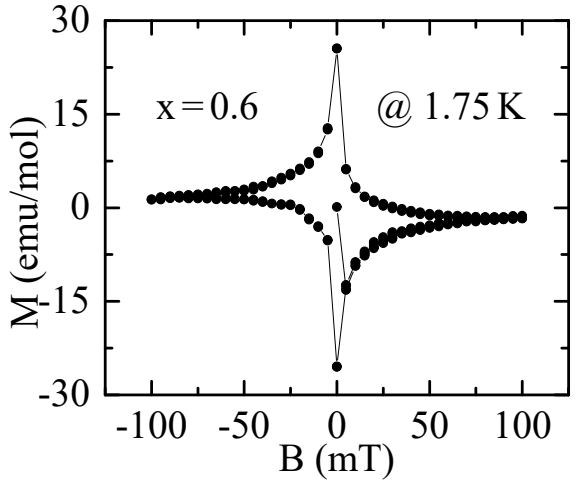


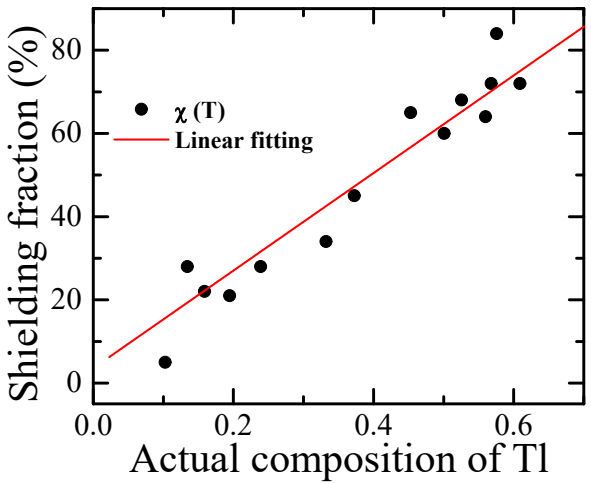


x = 0.6 is optimal for large volume fraction of the superconducting phase and structural stability

# Transport properties of $Tl_xBi_2Te_3$



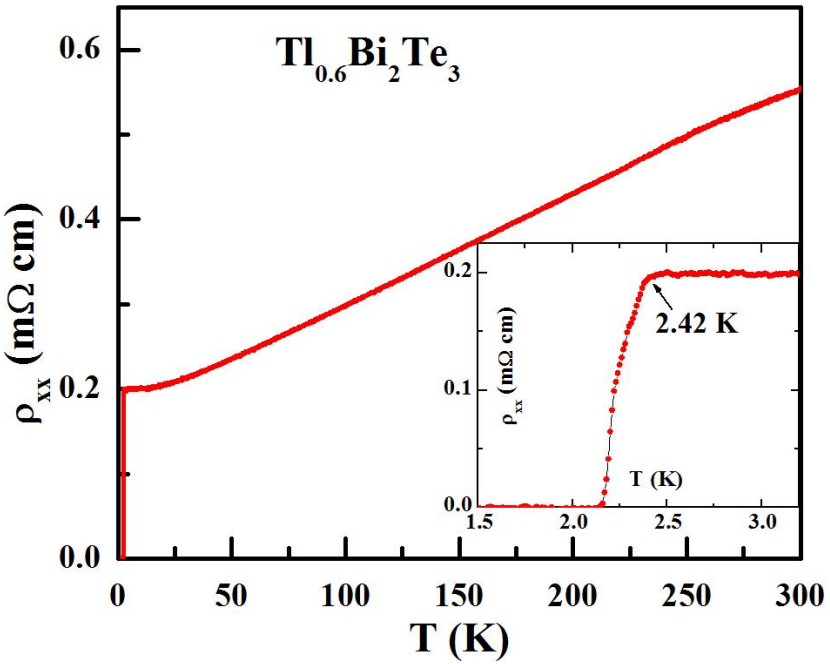


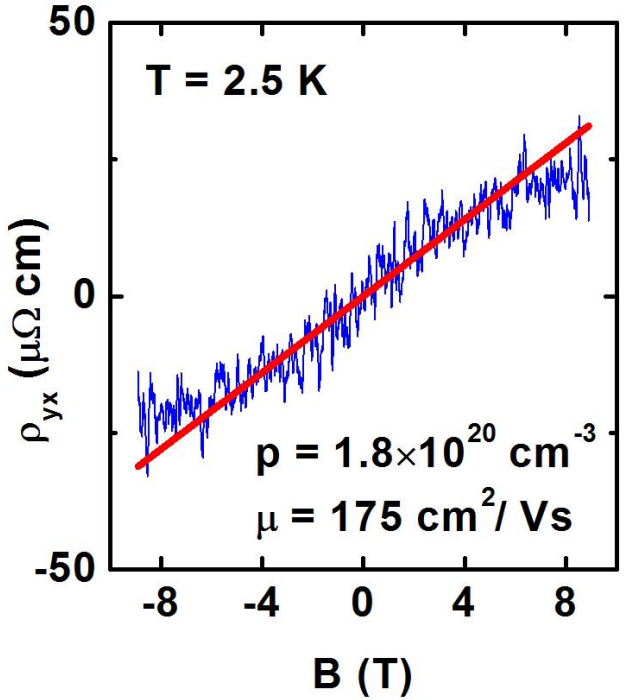


Electronic transport properties of $Tl_{0.6}Bi_2Te_3$

Z. Wang *et al*, *Chem. Mater.* (2016)

# Transport properties of $Tl_xBi_2Te_3$



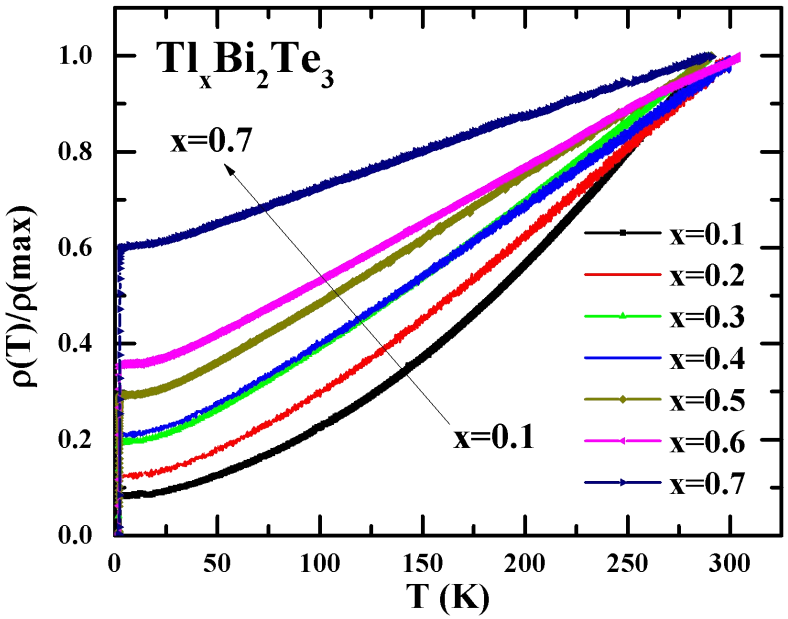


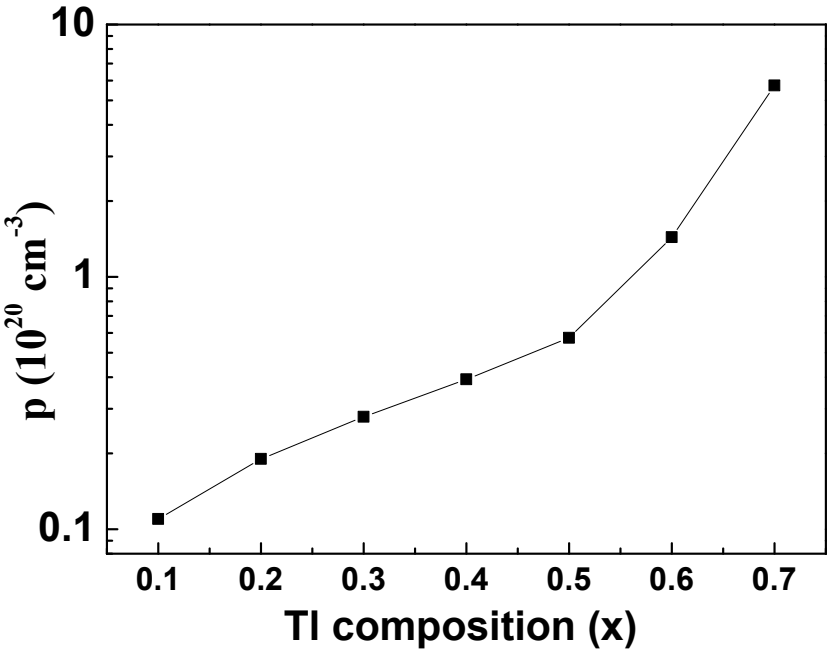


RRR decrease with increase of x;
scattering effect becomes stronger with x increase,

# Specific heat of $Tl_{0.6}Bi_2Te_3$

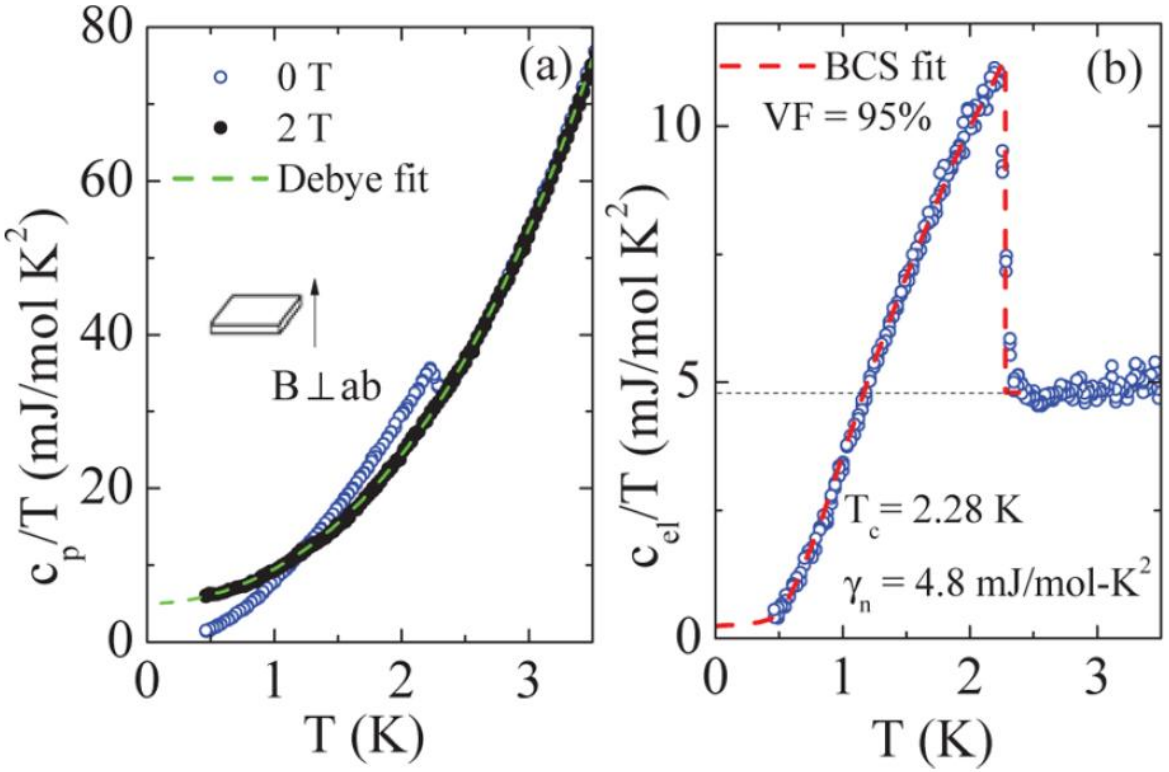


clear jump indicates bulk superconductor;
fully gapped;

Z. Wang *et al*, *Chem. Mater.* (2016)

# Upper critical field

$Tl_{0.6}Bi_2Te_3$

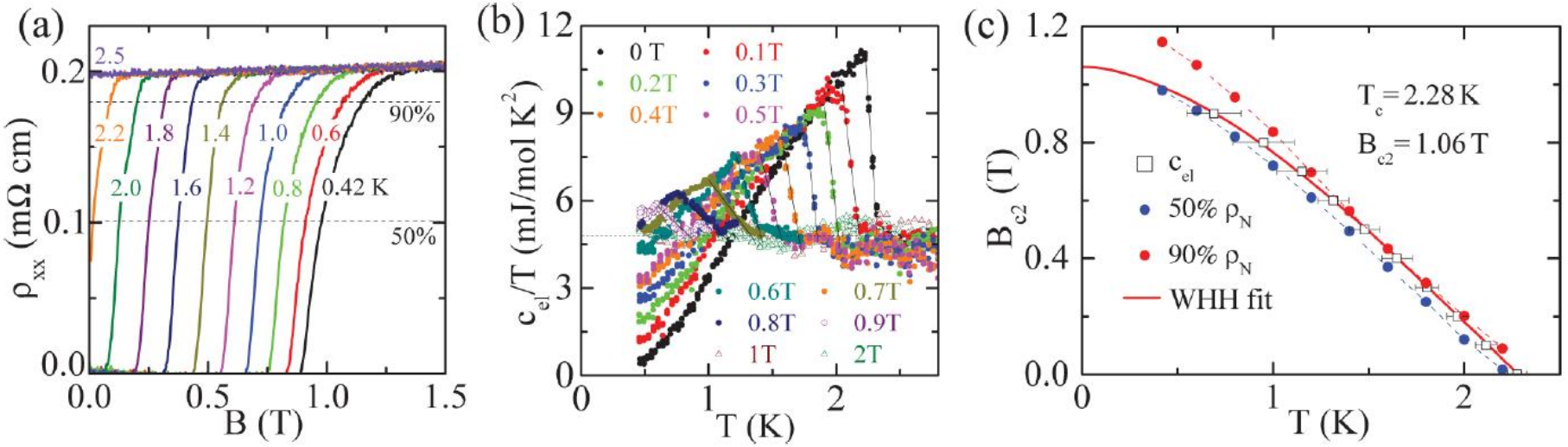


the specific data fit well to WHH theory,

$B_{c2}(0) = 1.06$ T; $\xi = 17.6$ nm,

the resistivity data point to a slightly unconventional temperature dependent

Z. Wang *et al*, *Chem. Mater.* (2016)

# 3. Exploration of topological superconductors

a) doping based on topological insulator

b) applied external pressure based on topological materials

# Background

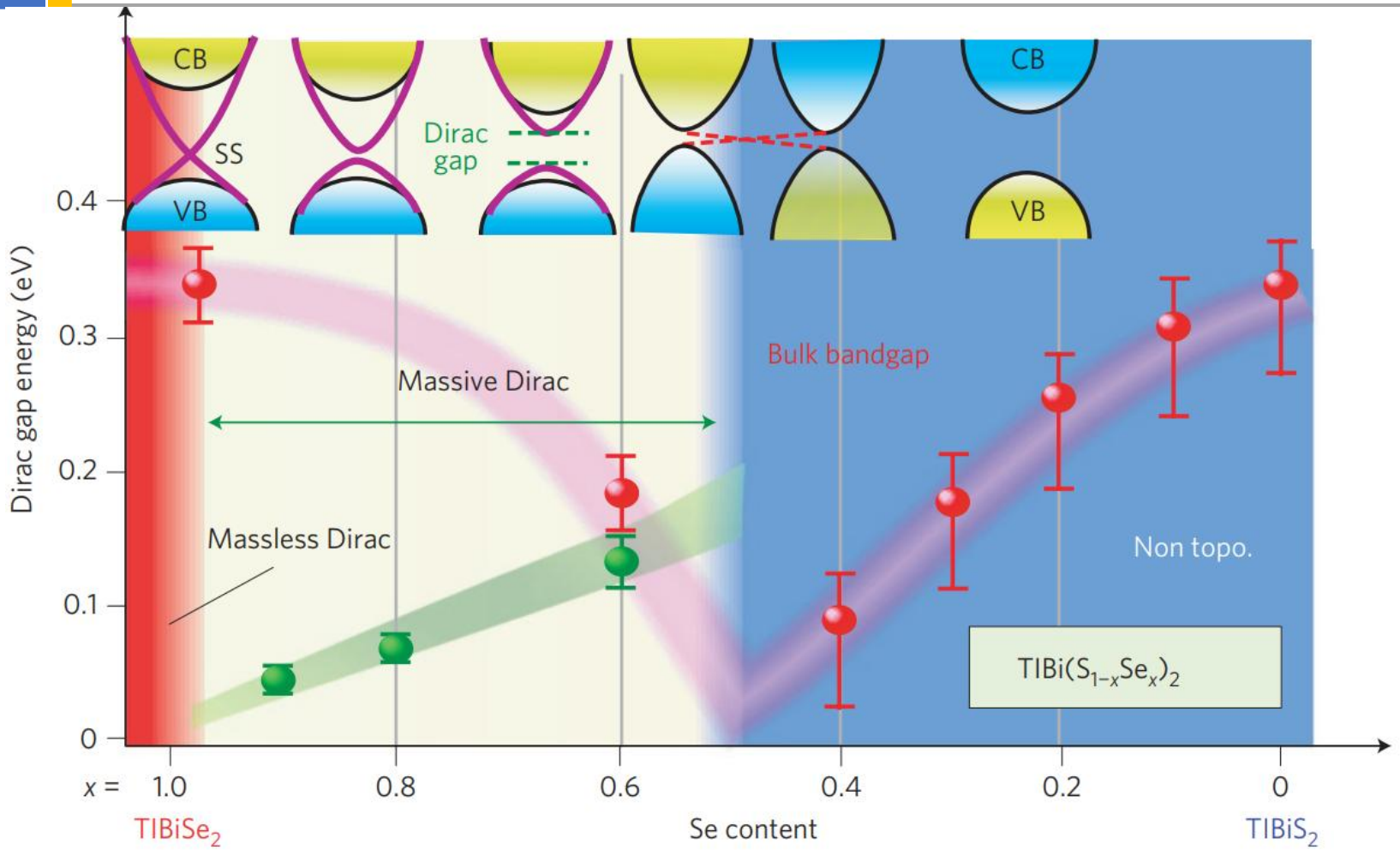


Electronic phase diagram of $TlBi(S_{1-x}Se_x)_2$

T. Sato et al, Nat. Phys., 7 (2011) 840

# Background

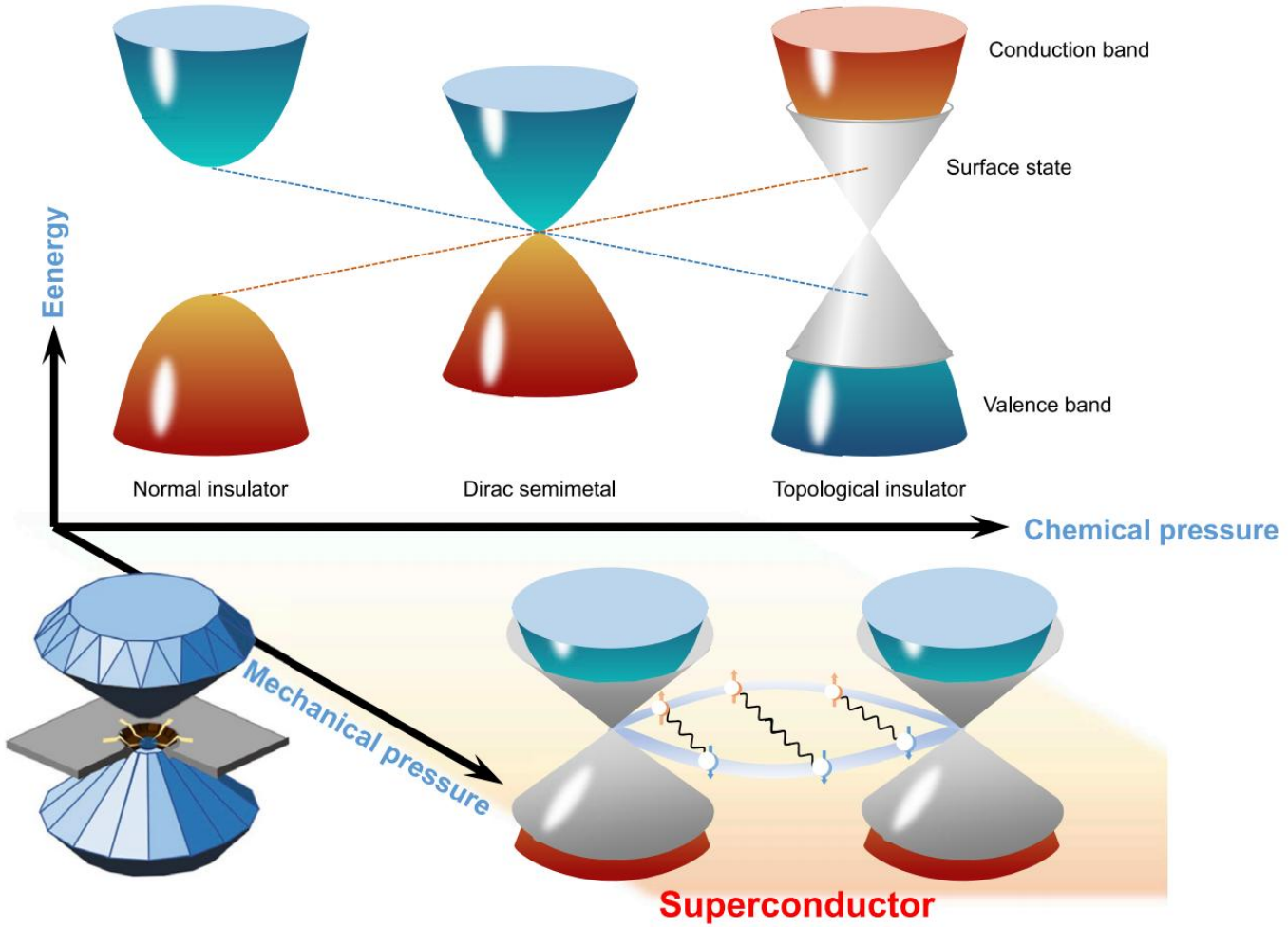


Schematic of chemical pressure and mechanical pressure effect on $TlBi(S_{1-x}Se_x)_2$ compounds

# Characterization of $TlBi(Se_{1-x}S_x)_2$

北京理工大學 BEIJING INSTITUTE OF TECHNOLOGY

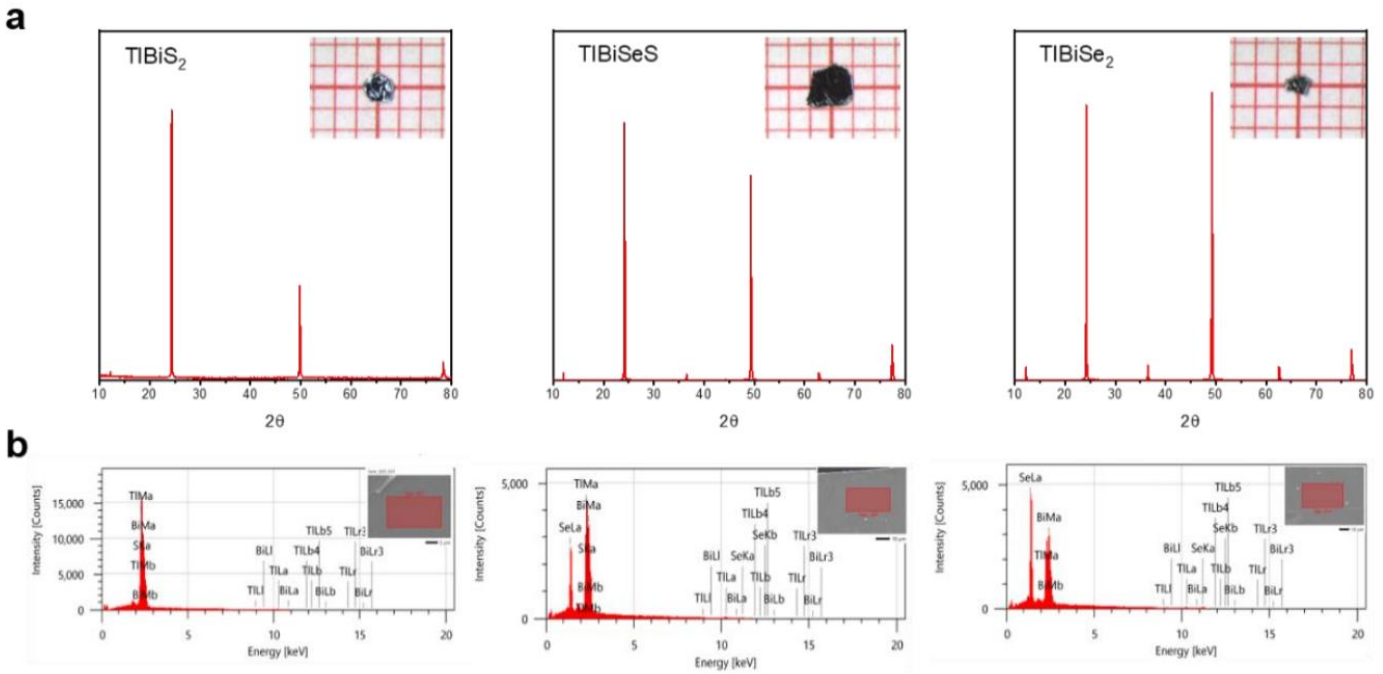


| Sample | Element | Ratio (atom%) | Sample | Element | Ratio (atom%) | Sample | Element | Ratio (atom%) |
|---|---|---|---|---|---|---|---|---|
| $TlBiS_2$ | S | 51.57 | TlBiSeS | S | 25.92 | $TlBiSe_2$ | Se | 52.20 |
| | Tl | 21.47 | | Se | 25.65 | | Tl | 19.88 |
| | Bi | 26.95 | | Tl | 20.34 | | Bi | 27.92 |
| | | | | Bi | 28.08 | | | |

XRD and EDS of $TlBi(Se_{1-x}S_x)_2$

C Pei, **ZW Wang**, Y P Qi, et al, Cell Reports Physical Science 3, 101094 (2022)

# Pressure induced superconductivity in $TlBi(Se_{1-x}S_x)_2$

北京理工大學 BEIJING INSTITUTE OF TECHNOLOGY

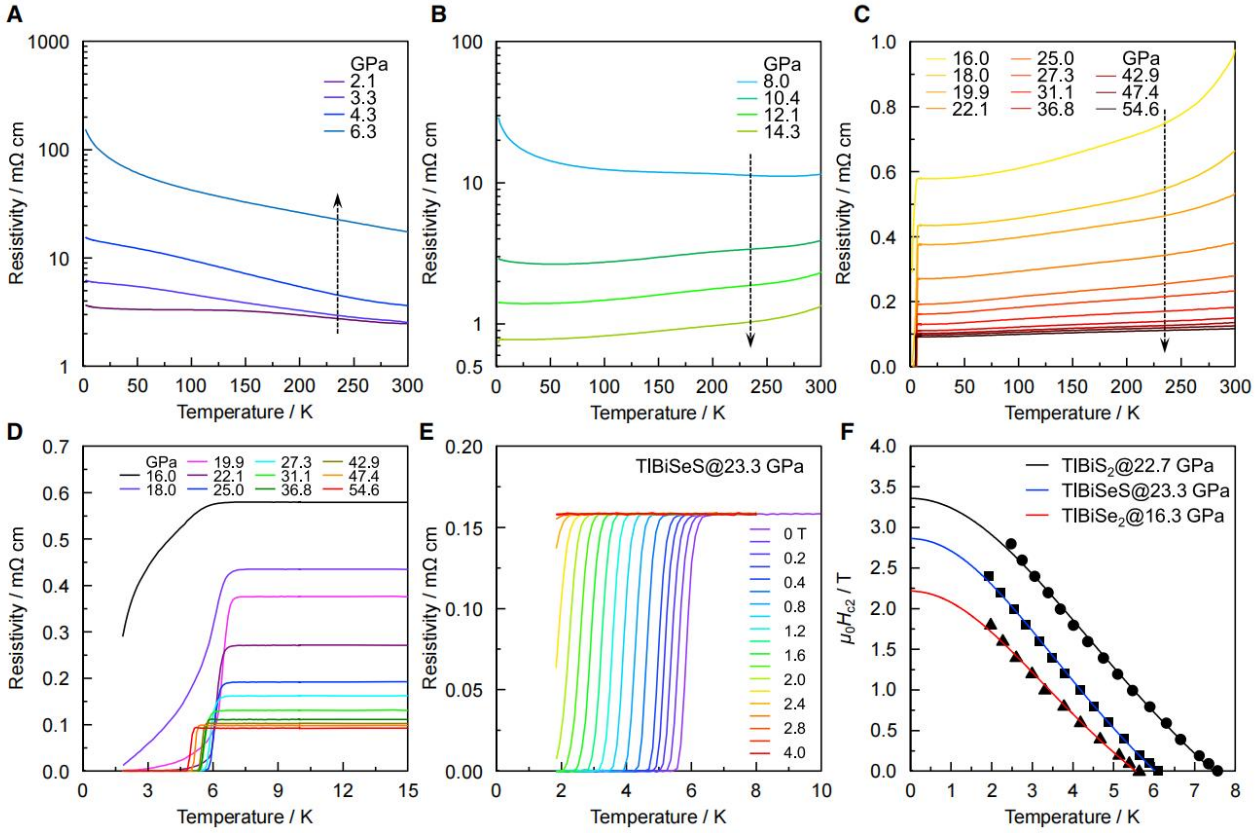


- The resistivity of TlBiSeS first increases with applied pressure and reaches the maximum value at 6.3 Gpa;
- Superconductivity appears at high pressure, and a maximum $T_c$ of 6.7 K is attained at p = 19.9 Gpa;
- a maximum $T_c$ of 8.1 and 6.0 K is observed in $TlBiS_2$ and $TlBiSe_2$

C Pei, **ZW Wang**, Y P Qi, et al, Cell Reports Physical Science 3, 101094 (2022)

# Evolution of crystal structure and Raman shift at high pressure

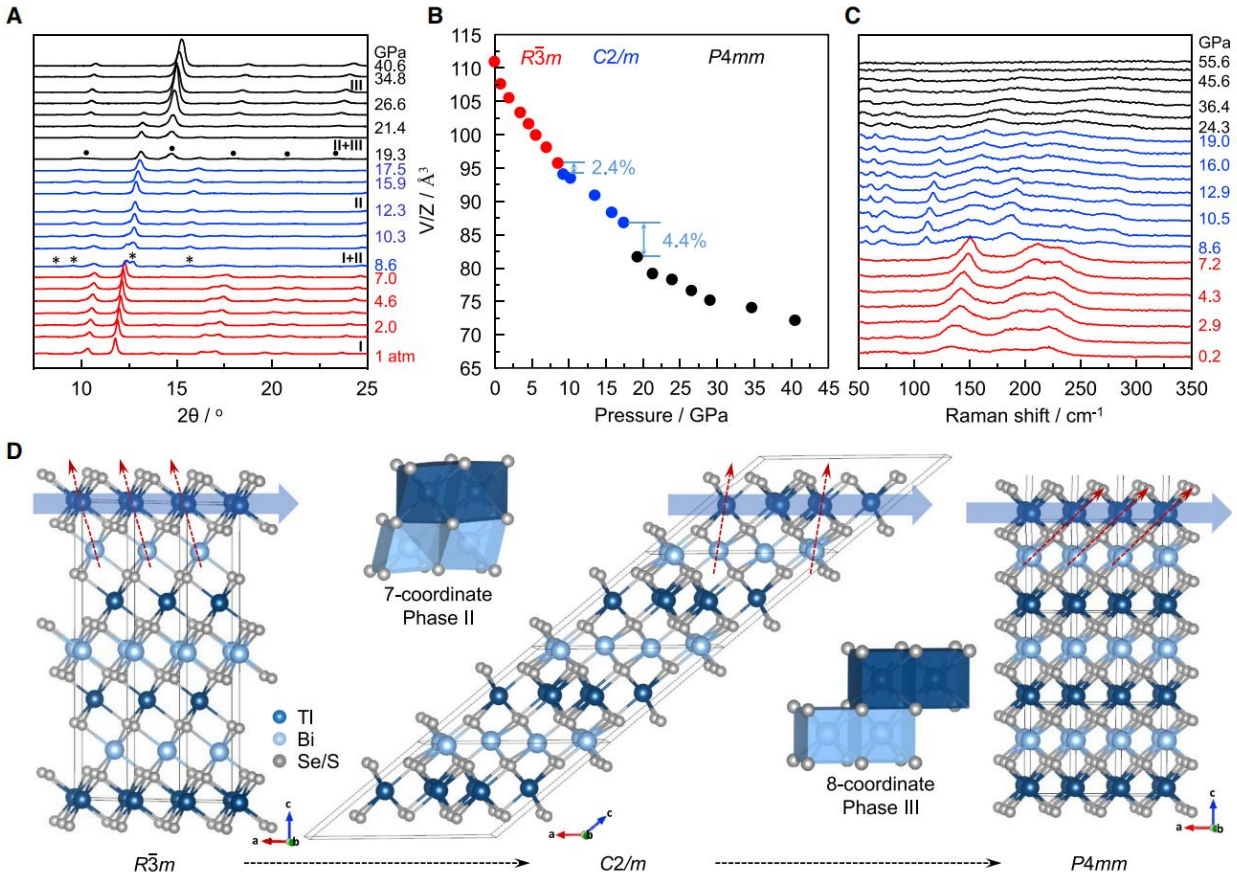


- phase transition appeared at about 9.1 GPa, and 21.3GPa, both from XRD and Raman measurements.
- Hexagonal-monoclinic-tetragonal phase transition at high pressure.

C Pei, **ZW Wang**, Y P Qi, et al, Cell Reports Physical Science 3, 101094 (2022)

# Phase diagram of $TlBi(Se_{1-x}S_x)_2$ at high pressure

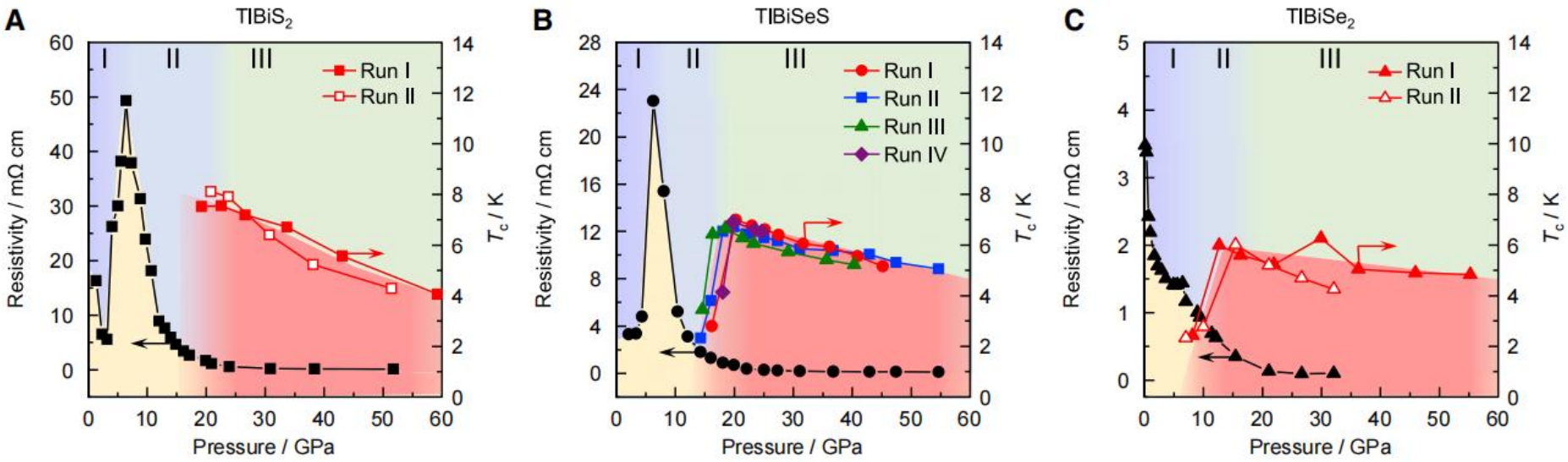


- high pressure dramatically alters both crystal and electronic structures of $TlBiS_2$, TlBiSeS, and $TlBiSe_2$.

C Pei, **ZW Wang**, Y P Qi, et al, Cell Reports Physical Science 3, 101094 (2022)

# Band calculation of $TlBi(Se_{1-x}S_x)_2$ at high pressure

北京理工大學 BEIJING INSTITUTE OF TECHNOLOGY

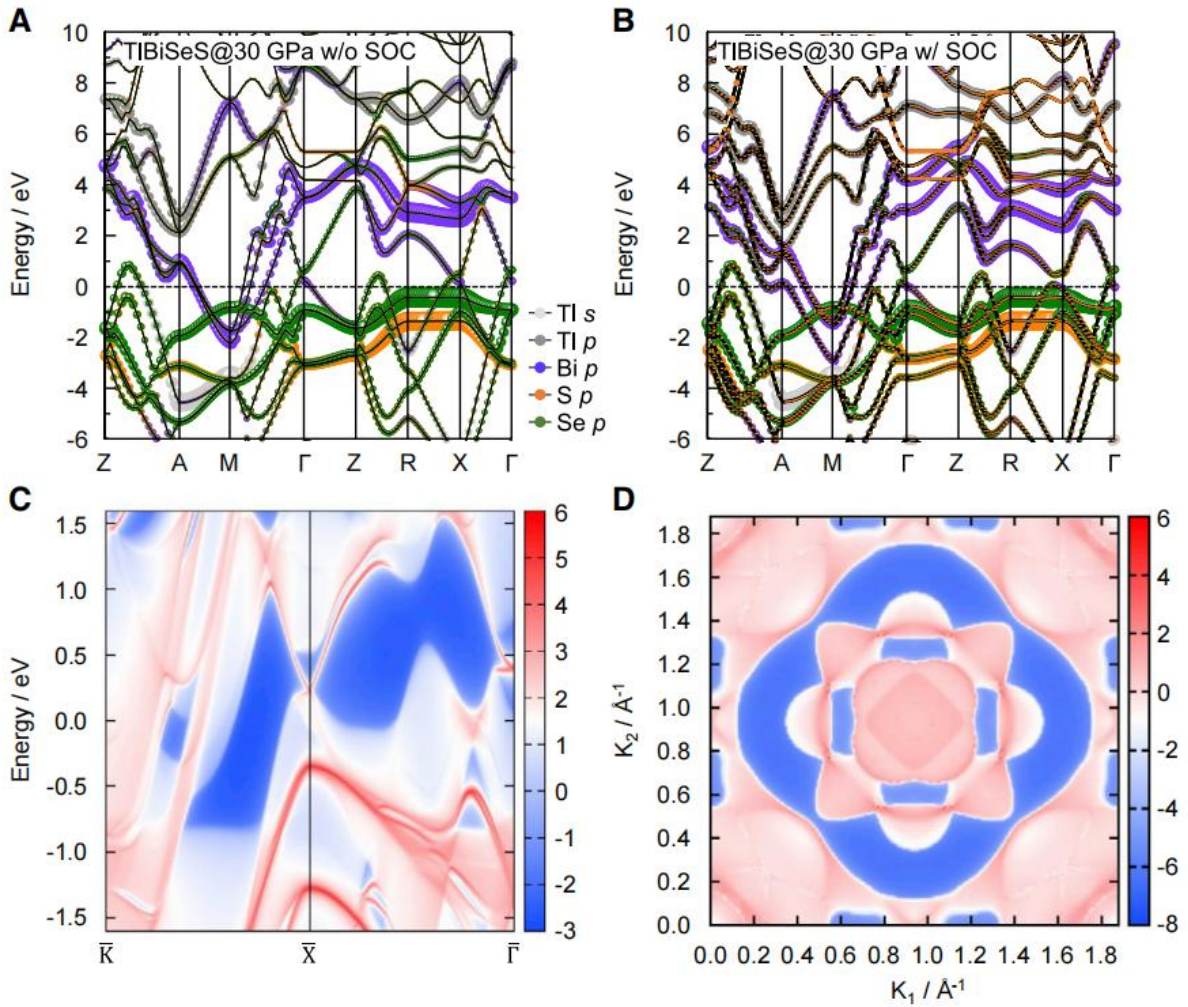


- there is an SOC-induced band inversion near the Fermi surface at the Γ and X points, the band gaps were approximately 688 and 662 meV, respectively.
- the $Z_2$ topological invariant
- Dirac-cone-like surface states of TlBiSeS at 30 GPa are located at 0.19 eV above Fermi level

C Pei, **ZW Wang**, Y P Qi, et al, Cell Reports Physical Science 3, 101094 (2022)

# Pressure induced superconductivity in $(PbSe)_5(Bi_2Se_3)_6$

北京理工大學 BEIJING INSTITUTE OF TECHNOLOGY

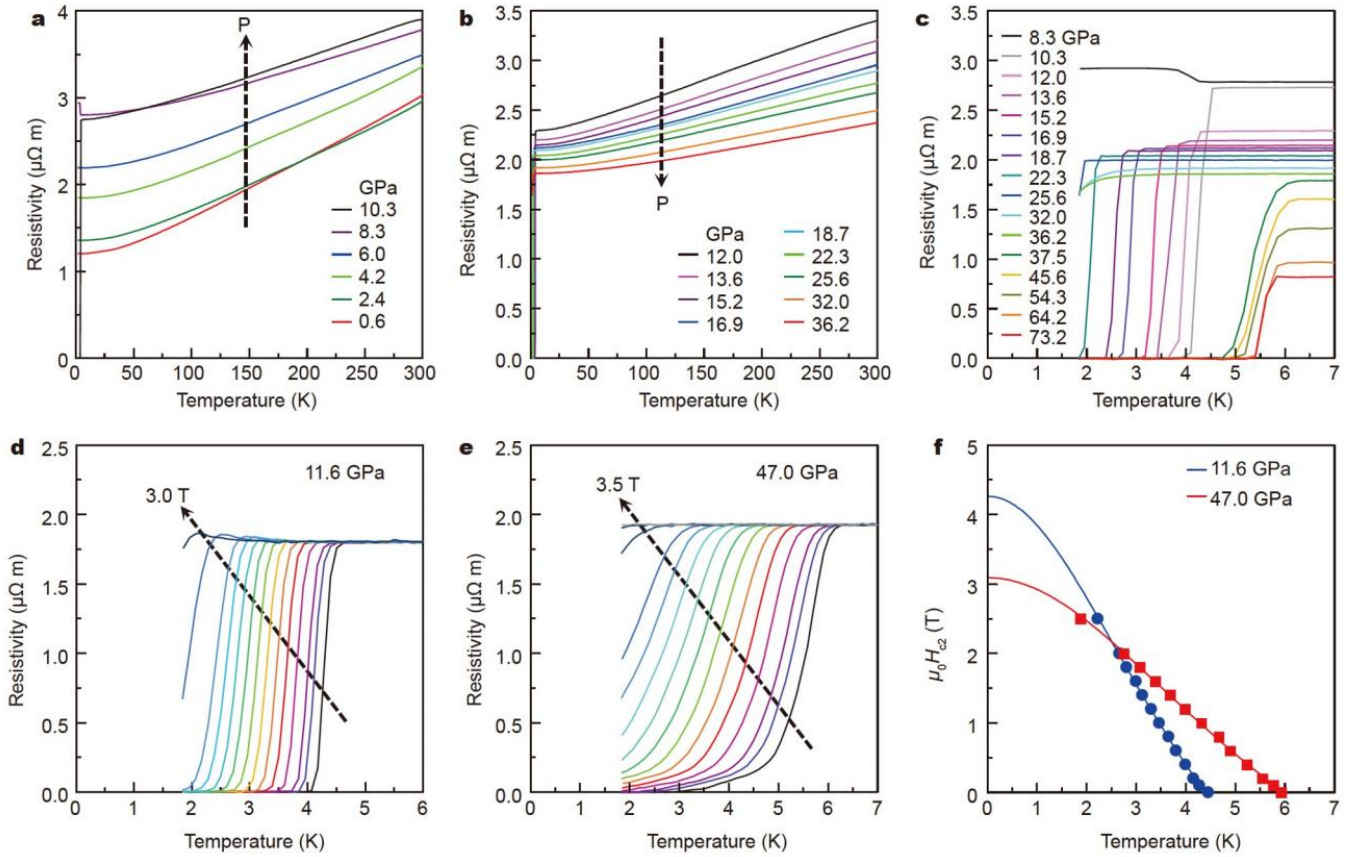


- a SC transition where resistivity reaches zero emerges at 4.6 K around 10 Gpa.
- the *Tc* onset is suppressed to a minimum of 1.9 K at around 25–30 GPa.
- increase rapidly with further increase in pressure above 32 GPa, reaching a value of 6.0 K at 37.5 GPa.

P Cui, **ZW Wang**, YP Qi, et al, SCIENCE CHINA Materials (2023)

# Evolution of crystal structure and Raman shift at high pressure

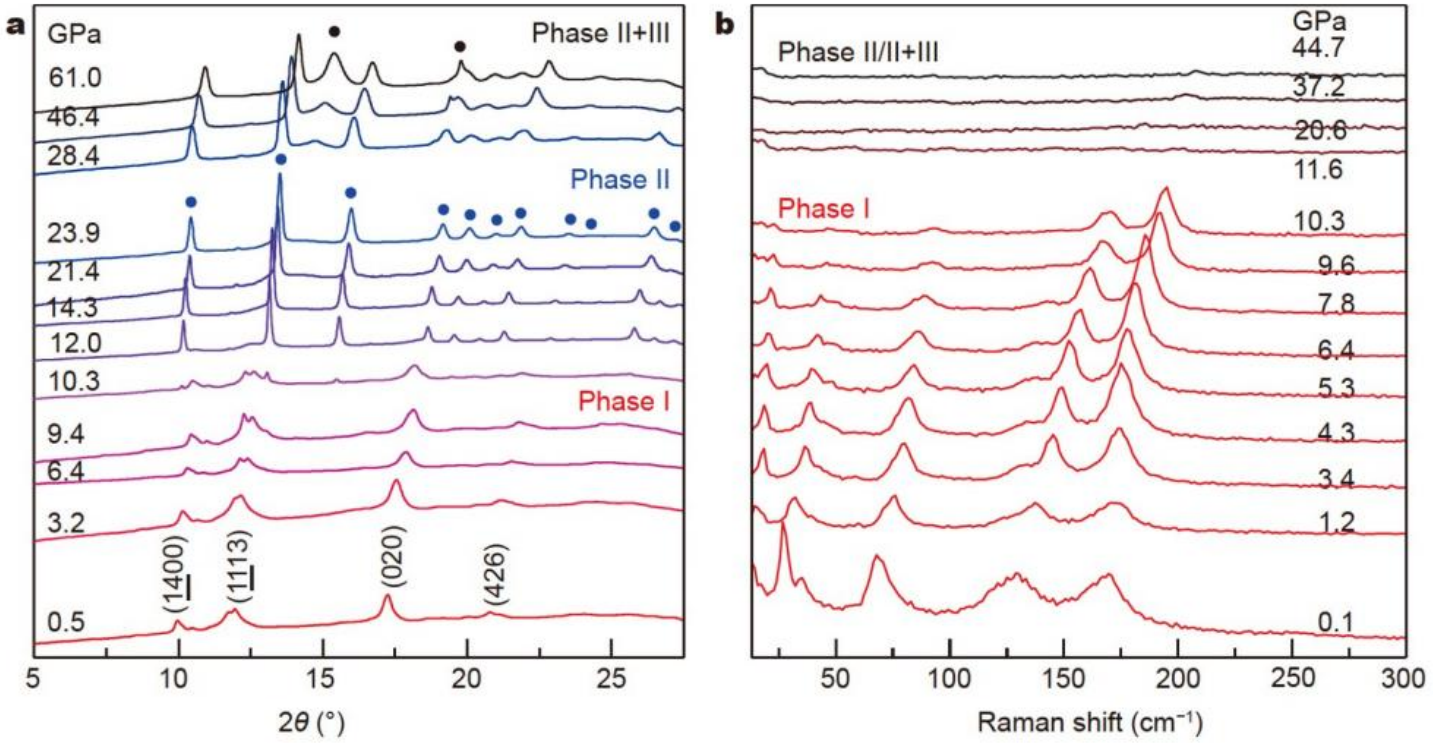


- *In-situ* XRD and Raman spectroscopy measurements demonstrate that two distinct high-pressure phases were achieved in $(PbSe)_5(Bi_2Se_3)_6$ upon compression

P Cui, ZW Wang, YP Qi, et al, SCIENCE CHINA Materials (2023)

# Phase diagram of $(PbSe)_5(Bi_2Se_3)_6$ at high pressure

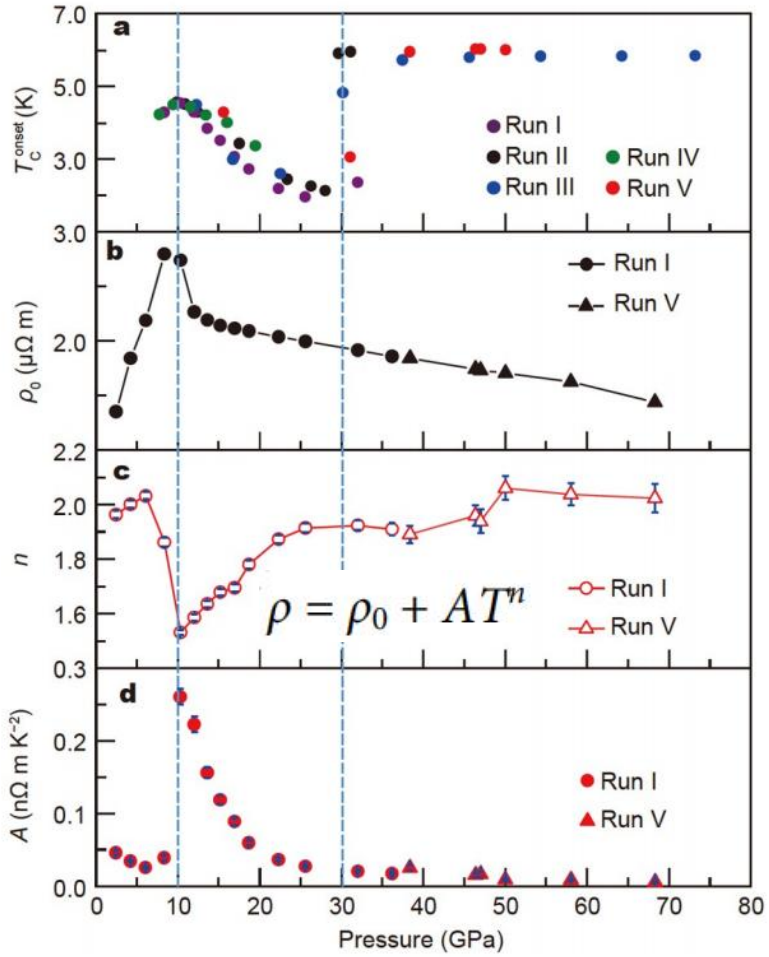


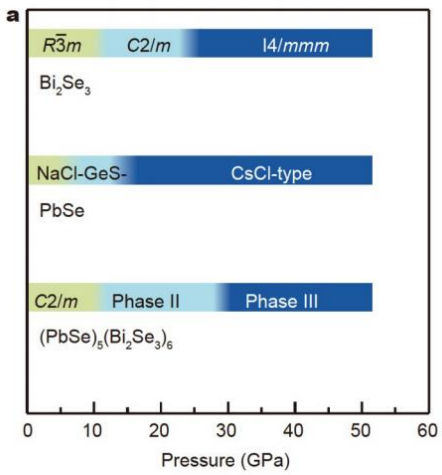


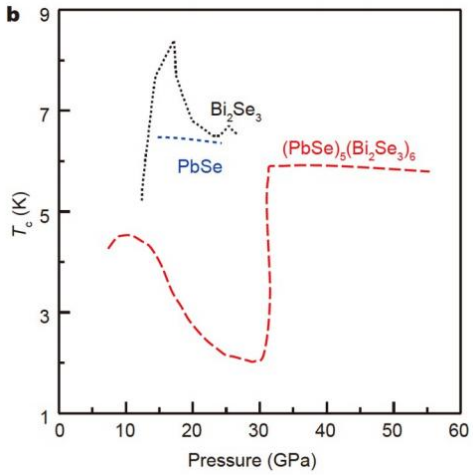


- In phase I, $\rho_0$ increases with pressure while $n$ maintains around 2, showing a Fermi-liquid behavior;
- In Phase II, a superconducting transition with $T_c$ ~ 4.6 K suddenly, however, $T_c$ is sensitive to pressure and decreases sharply upon compression.
- In Phase III, a new superconducting phase suddenly emerges, $T_c$ was enhanced as high as 6 K.

P Cui, ZW Wang, YP Qi, et al, SCIENCE CHINA Materials (2023)

# Outline

北京理工大學 BEIJING INSTITUTE OF TECHNOLOGY

- 1. Introduction of crystal and crystal growth
- 2. Crystal growth, physical properties of Kagome superconductors $AV_3Sb_5$
- 3. Exploration of topological superconductors
- 4. Summary

# 4 Summary

北京理工大學 BEIJING INSTITUTE OF TECHNOLOGY

1. Basic knowledge of crystal and crystal growth were presented;

2. Kagome superconductor $AV_3Sb_5$ single crystals were grown and their superconductivity and CDW were studied and manipulated;

3. A new superconductor TIxBi2Te3 was discovered and its superconductivity was characterized;

4. Possible TSC was induced by applying external pressure on two different types of topological materials.

# Acknowledgement

北京理工大學 BEIJING INSTITUTE OF TECHNOLOGY

## Collaborators:

| Theory | TEM | Transport | High pressure | biosensor | Crystal growth | ARPES | STM | ARPES |
|---|---|---|---|---|---|---|---|---|
|  |  | 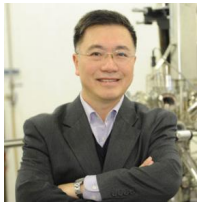 |  |  | 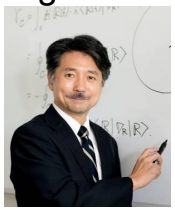 |  |  |  |
| Y.G. Yao | J.Q. Li | H.-H. Wen | Y.-P. Qi | J.-F. Han | Y. Ando | T. Sato | M.Z. Hasan | K. Okazaki |

## Students:


Yongkai Li


Jinjin Liu


Peng Zhu


Xin Zhang


Ying Yang


Liu Yang

## Funds:

国家自然科学基金委员会 NSFC

Ministry of science and technology of China 973 国家重点基础研究发展计划

北京市自然科学基金委员会办公室 Beijing Natural Science Foundation

BIT

# Thank you for your attention!